Published in final edited form as:
Nat Chem Biol. 2020 October 01; 16(10): 1120–1128. doi:10.1038/s41589-020-0592-z.

Development of a chemical probe against NUDT15

Si Min Zhang[#1], **Matthieu Desroses**[#1], **Anna Hagenkort**[#1], **Nicholas C.K. Valerie**[1], **Daniel Rehling**[2], **Megan Carter**[2], **Olov Wallner**[1], **Tobias Koolmeister**[1], **Adam Throup**[1], **Ann-Sofie Jemth**[1], **Ingrid Almlöf**[1], **Olga Loseva**[1], **Thomas Lundbäck**[3], **Hanna Axelsson**[3], **Shruti Regmi**[3], **Antonio Sarno**[4], **Andreas Krämer**[5], **Linda Pudelko**[1], **Lars Bräutigam**[1], **Azita Rasti**[1], **Mona Göttmann**[1], **Elisée Wiita**[1], **Juliane Kutzner**[6], **Torsten Schaller**[6], **Christina Kalderén**[1], **Armando Cázares-Körner**[1], **Brent D. G. Page**[1,7], **Rosa Krimpenfort**[8], **Saeed Eshtad**[8], **Mikael Altun**[8], **Sean G. Rudd**[1], **Stefan Knapp**[5], **Martin Scobie**[1], **Evert J. Homan**[1], **Ulrika Warpman Berglund**[1], **Pål Stenmark**[2,9], **Thomas Helleday**[1,10,*]

[1]Science for Life Laboratory, Department of Oncology-Pathology, Karolinska Institutet, Stockholm, Sweden

[2]Department of Biochemistry and Biophysics, Stockholm University, Stockholm, Sweden

[3]Chemical Biology Consortium Sweden, Science for Life Laboratory, Department of Medical Biochemistry and Biophysics, Karolinska Institutet, Stockholm, Sweden

[4]Department of Cancer Research and Molecular Medicine, Norwegian University of Science and Technology, Trondheim, Norway

[5]Institute of Pharmaceutical Chemistry, Goethe-University Frankfurt, 60438, Frankfurt, Germany

[6]Department of Infectious Diseases, University Hospital Heidelberg, Heidelberg, 69120, Germany

[7]Faculty of Pharmaceutical Sciences, University of British Columbia, Vancouver, Canada

[8]Division of Translational Medicine and Chemical Biology, Department of Medical Biochemistry and Biophysics, Karolinska Institutet, Stockholm, Sweden

[9]Department of Experimental Medical Science, Lund University, Lund, Sweden

[10]Weston Park Cancer Centre, Department of Oncology and Metabolism, University of Sheffield, S10 2RX Sheffield, UK

[*]**Corresponding Author:** Correspondence and requests for materials should be addressed to Prof. Thomas Helleday, Science for Life Laboratory, Karolinska Institutet, Box 1031, SE-171 21 Stockholm, Sweden, thomas.helleday@scilifelab.se.

Author Contributions

T.H. devised the concept of the study. T.H., P.S., S.G.R., and U.W.B. supervised the project. A.H., S.M.Z., N.C.K.V., M.G., A.C-K., R.K., S.E., M.A., T.S., L.P., L.B., A.R., and J.K. designed, performed and analyzed biological experiments. M.D., O.W., A.T., T.K., E.J.H., and M.S. designed, performed and analyzed medicinal chemistry experiments. M.C., D.R., and P.S. designed, performed and analyzed structural biology experiments. O.L., A-S.J., I.A., C.K., A.K., E.W., B.D.P.G., and S.K. designed, performed and analyzed biochemistry experiments. T.L., H.A. and S.R. designed, performed and analyzed biochemical screening campaign. E.J.H. performed computational chemistry analysis. A.S. designed, performed and analyzed the mass-spectrometry experiments. S.M.Z. compiled data; S.M.Z., M.D., A.H., T.H., and N.C.K.V. prepared the manuscript. S.M.Z., M.D., and A.H. contributed equally to the work. All authors discussed results and approved the manuscript.

Conflict of Interest Statement

The authors declare no conflict of interest.

Europe PMC Funders Author Manuscripts

[#] These authors contributed equally to this work.

Abstract

The NUDIX hydrolase NUDT15 was originally implicated in sanitizing oxidized nucleotides but was later shown to hydrolyze the active thiopurine metabolites, 6-thio-(d)GTP, thereby dictating the clinical response of this standard-of-care treatment for leukemia and inflammatory diseases. Nonetheless, its physiological roles remain elusive. Here, we sought to develop the first small-molecule NUDT15 inhibitors to elucidate its biological functions, and potentially for improving NUDT15-dependent chemotherapeutics. Lead compound TH1760, demonstrated low-nanomolar biochemical potency through direct and specific binding into the NUDT15 catalytic pocket and engaged cellular NUDT15 in the low-micromolar range. We further employed thiopurine potentiation as a proxy functional read-out and demonstrated that TH1760 sensitized cells to 6-thioguanine through enhanced accumulation of 6-thio-(d)GTP in nucleic acids. A biochemically validated, inactive structural analog, TH7285, confirmed that increased thiopurine toxicity is *via* direct NUDT15 inhibition. In conclusion, TH1760 represents the first chemical probe for interrogating NUDT15 biology and potential therapeutic avenues.

Keywords

NUDT15; TH1760; small molecule inhibitor; thiopurines; acute lymphoblastic leukaemia; 6-thio-dGTP

Introduction

In the cell, nucleotides are vulnerable to enzymatic and non-enzymatic modification, which, if left unattended, may have dire consequences on genome integrity and cellular fitness. Fortunately, the presence of “housekeeping” or “sanitation” enzymes effectively remove these species to limit their detrimental effects[1,2]. The nucleoside diphosphate linked to moiety X (NUDIX) hydrolase superfamily is among the most prominent of this group, defined by the shared NUDIX box motif (Gx5Ex5[UA]xREx2EExGU; U, aliphatic, hydrophobic residue; x, any residue) that comprises their enzymatic core[3]. The variety in their substrate recognition sites ensures broad substrate diversities among the human NUDIX proteins and, likely, importance for distinct biological functions[4].

NUDIX-type 15 (NUDT15) is homologues to NUDT1 (MutT homologue 1, MTH1) and thus has previously been referred to as MTH2. Early studies focused on its role as a redundancy factor for MTH1 by hydrolyzing the potentially mutagenic guanine species, 8-oxo-dGTP[5–7]. While some evidence indicated its involvement in oxidized nucleotide metabolism, detailed biochemical and structural work by our group and others have concluded that NUDT15 has approximately 40-fold lower enzymatic activity against 8-oxo-dGTP as compared to MTH1[8]. Other suggested functions of NUDT15 include cleaving 7-methyl-GMP and 7-methyl-GDP from methylated, capped mRNA and thereby potentially regulating mRNA stability[9]; and stabilizing polymerase clamp PCNA (proliferating cell nuclear antigen) from degradation[10]. Although these findings have provided important clues,

Europe PMC Funders Author Manuscripts

at this time, the physiological function(s) of NUDT15, in nucleotide pool maintenance/sanitization and beyond, have yet to be comprehensively elucidated.

Meanwhile, recent clinical studies have observed that missense mutations, such as R139C, in NUDT15 are significantly correlated with elevated hematopoietic toxicity among patients receiving thiopurine-based therapies (6-thioguanine, 6-mercaptopurine and azathioprine)[11–16]. Thiopurines are a group of cytotoxic guanosine analogue antimetabolites that are routinely used to treat leukemia (e.g. acute lymphoblastic leukemia, ALL; acute myeloid leukemia, AML) and inflammatory diseases (e.g. Crohn's disease)[17–21]. In cells, thiopurines are tri-phosphorylated into 6-thio-(d)GTP before being mis-incorporated into genomic material, thereby inducing futile DNA repair and eventually cell death[22–26]. Moreover, 6-thio-dGTP can be preferentially incorporated into *de novo* synthesized telomeres in telomerase-expressing malignant cells, resulting in selective telomere dysfunction and cytotoxicity in cancerous *versus* normal tissue-derived cell lines[27,28].

Interestingly, mechanistic studies focusing on NUDT15-related thiopurine hypersensitivity have revealed that 6-thio-(d)GTP are efficient substrates for NUDT15 hydrolysis[8,16,29]. Depletion of NUDT15 in cells and *in vivo* could effectively elevate 6-thio-(d)GTP accumulation and incorporation, and the subsequent cellular responses leading to apoptosis[16,29]. Translating to a therapeutic perspective, a 20-fold reduction of thiopurine dosage could be achieved in NUDT15 knockout mice without sacrificing anti-leukemic efficacy, indicating that the current thiopurine-based therapies could be potentially modulated through targeting the 6-thio-(d)GTPase activity of NUDT15[30].

To interrogate the substrate(s)/activit(ies) of NUDT15 and to provide potential tool for improving antimetabolite therapeutics subject to NUDT15 metabolism (e.g. thiopurines, 6-thio-dGTP), herein, we sought to develop potent and selective small molecule NUDT15 inhibitors. Our lead compound inhibited NUDT15 at low-nanomolar biochemical IC_{50} through direct binding into the NUDT15 catalytic pocket and further demonstrated on-target binding in cells. We then evaluated and confirmed the in-cell activity of our lead by its ability to target the 6-thio-(d)GTPase activity of NUDT15 and thereby potentiate thiopurine-induced cytotoxicity. The use of an inactive analog validated that increase of thiopurine toxicity is a direct result of NUDT15 enzymatic inhibition. We herein report the first *bona fide* chemical probe against NUDT15.

Results

Screening and development of NUDT15 inhibitors

To develop potent and selective small molecule NUDT15 inhibitors as a chemical probe to understand NUDT15 biology, we first established a biochemical screening campaign utilizing our previously reported enzyme-coupled malachite green (MG) assay (Fig. 1a) [8,29]. In this assay, human recombinant NUDT15, dGTP (a known NUDT15 substrate)[29], and *E. coli* inorganic pyrophosphatase (PPase) were combined. In short, dGTP is first hydrolyzed by NUDT15 to dGMP and pyrophosphate, then the released pyrophosphate is converted by PPase to inorganic phosphate that was subsequently detected with the MG reagent and used as an enzymatic activity read-out for NUDT15 activity. Utilizing this MG assay-based

screening platform, 17946 distinct chemical entities with commercial (Enamine) or in-house (donated by Biovitrum AB[31]) origins were screened at a single concentration of 10 μM (Fig. 1a; Supplementary Table 1). The screening performance was deemed excellent with an average z' factor of 0.87, and the hit identification criterion was defined as three times the standard deviation beyond the average inhibition for the screening library (Supplementary Fig. 1), as defined previously[32]. Based on their inhibitory potency, potential binding efficiency, and druggability, 37 hit compounds were selected for follow-up dose-response validation of their inhibitory potency. Compound **1** (TH884) exhibited good inhibitory potency against NUDT15 (MG assay IC_{50} = 7 μM) and was chosen as a promising chemical starting point for further inhibitor development (see Supplementary Fig. 2 for inhibitor screening funnel).

As the first step of NUDT15 inhibitor optimization, we developed a concise synthetic route and initiated structure-activity relationship (SAR) studies of the hit compound TH884, where chemical features critical for efficacy were identified by MG assay inhibitory potency. Initial SAR studies focused on the phenyl part (Supplementary Table 2). Removal of the fluorine atom (**2**) or replacing the phenyl ring by non-aromatic hydrophobic moieties (**3** and **4**) was well tolerated, removal of the phenyl moiety resulted in an IC_{50} > 100 μM (**5**); indicating that although the phenyl ring is not critical for activity, occupancy of this area by a hydrophobic group was required for NUDT15 inhibition. Noting a slightly improved IC_{50} with the carbamate **4**, we next installed a carbonyl between the piperazine and the phenyl (compound **6**), resulting in more than 30-fold improvement of potency compared to hit compound TH884. In contrast, extension of this linker strongly reduced potency (**7** and **8**). Substitution of the phenyl ring of compound **6** in *ortho*, *meta* and *para* positions (**9**, **10**, and **11**) further enhanced activity, particularly, the 4-bromo analogue **11**, which led to 4-fold improvement over **6**. Other *para* substituents including methyl (**12**), amino (**13**), cyano (**14**), methanesulfonyl (**15**), or guanidine (**16**) failed to further improve potency of compound **6**. Finally, while the presence of a benzofuran ring (**17**) did not increase the efficacy substantially, replacement of the phenyl ring by an indole led to discovery of the lead compound **18** (TH1760), which demonstrated more than 200-fold improvement in biochemical potency compared to hit compound TH884 in inhibiting the hydrolysis of dGTP (MG assay IC_{50} = 25 nM *vs* 7 μM, Fig. 1b) or the preferred substrate of NUDT15, 6-thio-dGTP (IC_{50} = 57 nM *vs* 12.5 μM, Extended Data 1). Further SAR work (Supplementary Table 3) showed that the sulfonamide function is necessary for activity; its conversion to an amide abrogated activity (**19**). Replacement of the indolyl-amide carbonyl by a urea linker (**20**) or its removal (**21**), both reduced potency.

We further interrogated the selectivity of the lead compound TH1760. When tested at 100 μM (approximately 4000-fold above IC_{50} against NUDT15), TH1760 showed impressive selectivity over a panel of related proteins with sequential or functional resemblance to NUDT15, including other human NUDIX proteins (MTH1, NUDT2, NUDT5, NUDT9, NUDT12, NUDT14, NUDT18 and NUDT22) and nucleotide pyrophosphatases (dCTPase, dUTPase and ITPase) (Fig. 1c). The selectivity of TH1760 was further scrutinized and confirmed with the Eurofins Cerep SafetyScreen44™ Panel and a curated library of 44

kinases, where TH1760 at 10 or 12 μM, respectively, did not demonstrate significant interaction and/or inhibition of the tested targets (Extended Data 2).

We next confirmed that TH1760 inhibited NUDT15 through a direct interaction, by monitoring NUDT15 thermal stability using the differential scanning fluorimetry (DSF). Incubation with TH1760 stabilized NUDT15 from heat-induced unfolding and increased its melting temperature by >10 °C in a dose-dependent manner over the DMSO control (Fig. 1d). Meanwhile, the initial hit compound TH884 could not substantially alter NUDT15 stability, indicating that the improved potency of TH1760 was owing to its increased affinity to NUDT15.

Structural insight into NUDT15 inhibitor development

To gain further insight into the inhibitory mechanism of TH1760, we determined the structure of NUDT15 co-crystalized with TH1760 at a resolution of 1.6 Å (Fig. 2a, Supplementary Fig. 3a). TH1760 binds deep in the substrate pocket of NUDT15 in a similar orientation as 6-thio-GMP (PDB ID: 5LPG)[2]. Similarly to the guanine of 6-Thio-GMP, the benzoxazolone moiety of TH1760 also forms a direct hydrogen bond with the peptide backbone of Gly137 (Fig. 2b). TH1760 further forms another two hydrogen bonds with NUDT15: firstly, between the carbonyl group of the benzoxazolone moiety and the backbone of Leu138; and secondly, between the sulfonamide group and Thr94, which only interacted with 6-thio-GMP *via* a coordinated water molecule. Additionally, the amide oxygen and the indole nitrogen of TH1760 engage in water-mediated interactions with Arg34 and Glu88, respectively, with the latter further strengthened by a perpendicular pi-stacking interaction between the aromatic rings of the indole group and Tyr90 (Fig. 2c). These additional interactions observed in the NUDT15-TH1760 complex, but not in the NUDT15-6-thio-GMP structure, likely confer TH1760 with a higher binding affinity to NUDT15 than 6-thio-GMP.

From the binding modality between TH1760 and NUDT15, we next developed an inactive analogue of TH1760 to serve as a negative control. As the benzoxazolone moiety of TH1760 fits tightly into the NUDT15 substrate pocket, we rationalized that N-methylation of the benzoxazolone would create steric hindrances and compromise binding to NUDT15 (Supplementary Fig. 3b). As predicted, the resulting compound **22** (TH7285) could not stabilize NUDT15 from heat-induced denaturation, suggesting a loss of direct binding to NUDT15; and furthermore, abolished inhibition of the dGTPase (MG assay IC_{50} > 100 μM) (Fig. 2d-e) and 6-thio-dGTPase (Extended Data 1) activities of NUDT15.

Cellular engagement of NUDT15 by lead compound TH1760

To determine if the biochemical potency of TH1760 could be translated to the cellular context, we next evaluated TH1760 with two orthogonal cellular target engagement assays using both endogenous and HA-tagged NUDT15. Epitope tagging was preferred to ensure accurate detection of NUDT15 protein with higher affinity antibodies. The cellular thermal shift assay (CETSA) is based on the principle that ligand binding could alter protein thermal stability and hence its aggregation temperature (T_{agg}) upon heating [33]. In the assay, intact HL-60 cells overexpressing HA-tagged NUDT15 were treated with the hit compound

TH884, the lead TH1760, its inactive analogue TH7285, or DMSO control prior to heating at increasing temperatures. Detection of the remaining soluble NUDT15 *via* western blot demonstrated that only TH1760, but not TH884 or TH7285, significantly affected the thermal stability of cellular NUDT15 by dose-dependently increasing the apparent T_{agg} by up to ~6.5 °C (Fig. 3a). Isothermal dose response fingerprint (ITDRF) CETSA in intact NB4 cells or its lysate further confirmed that TH1760 substantially stabilized NUDT15 from 10 μM (Supplementary Fig. 4). Alternatively, TH1760 was subjected to the Drug Affinity Responsive Target Stability (DARTS) assay[34], which assesses target engagement based on resistance to protease digestion. In agreement with CETSA, TH1760, but not the inactive analogue TH7285, protected endogenous and HA-tagged NUDT15, respectively, from pronase digestion when applied to U2OS cell lysate (Fig. 3b) or intact HCT116 cells (Fig. 3c). Collectively, these data strongly suggest that TH1760 is a cell-active inhibitor of NUDT15.

Inhibition of cellular NUDT15 by TH1760

Having demonstrated the on-target binding of the lead NUDT15 inhibitor TH1760, we next sought to determine if TH1760 also exhibits in-cell functional activity. However, loss of NUDT15 activity has yet to be linked to any robust phenotype, hampering inhibitor evaluation based on its physiological functions. We instead exploited the role of NUDT15 in controlling thiopurine efficacy by converting 6-thio-(d)GTP back to the inactive species, 6-thio-(d)GMP. We reasoned that in-cell inhibition of NUDT15 could be evaluated by the phenotype of thiopurine potentiation (Fig. 4a).

Thiopurines, mainly 6-thioguanine (6-TG) and mercaptopurine (6-MP), are routinely administered to treat ALL, AML and CML[18–21], hence the AML cell lines HL-60 and NB4 were employed as the experimental model in this study. Consistent with the literature, NUDT15 knockdown in NB4 and HL-60 cells *via* shRNA substantially decreased the thiopurine concentrations required to inhibit 50% of cell proliferation (EC_{50}) (Fig. 4b; Extended Data 3a-b); while no significant effect on DNA replication was caused by knockdown alone (Extended Data 3c-d). Critically, the observed thiopurine sensitization could only be attenuated by overexpressing shRNA-resistant wildtype (WT) but not catalytically dead (NUDT15 E67A; CD)[35] or unstable (NUDT15 R139C; US)[29] NUDT15 protein, thus validating thiopurine potentiation as a read-out for NUDT15 catalytic activity (Fig. 4c; Extended Data 3e-h).

Next, NB4 and HL-60 cells were treated with a dose-matrix of thiopurine (6-TG or 6-MP) and TH1760 before cell viabilities were determined by resazurin assay and synergy score calculated. While TH1760 alone minimally altered DNA replication, proliferation, or viability up to 100 μM, it displayed strong synergistic killing when combined with thiopurines and dose-dependently reduced the EC_{50} values by up to ~10-fold, mirroring the sensitivity seen with NUDT15 knockdown (Fig. 5a-b; Supplementary Fig. 5a-e). The percentage of sub-G1 cells, an indicator of cell death, followed the same trend (Supplementary Fig. 5f-i). To validate that the observed effects were not restricted to certain cell lines, the TH1760-induced thiopurine sensitization was further shown with a panel of hematological cell lines (Fig. 5c; Extended Data 4a-b).

To confirm that TH1760 potentiated thiopurines through inhibiting NUDT15, we next applied 6-TG, with or without TH1760, to NB4 cells with conditional NUDT15 knockdown. TH1760 demonstrated consistent dose-dependent potentiation of 6-TG in NUDT15-proficient cells, which, however, was abrogated upon NUDT15 depletion (Fig. 5d; Extended Data 4c). Furthermore, TH7285, the inactive analogue of TH1760, could not sensitize cells to 6-TG, further underscoring that TH1760 potentiates thiopurine cytotoxicity in a NUDT15-dependent manner (Fig. 5e; Extended Data 4d-e).

Emerging resistance to anticancer antimetabolites remains a major barrier to effective disease control. We next investigated the potential of TH1760 in overcoming thiopurine resistance. Here we first combined TH1760 with 6-TG treatment in HCT116 cells, a colorectal carcinoma cell line exhibiting 6-TG resistance due to defective mismatch repair (MMR) machinery[24], along with its MMR-restored counterpart HCT116 3-6 cells. TH1760 effectively sensitized both cell lines to 6-TG, mirroring the effect of shRNA-guided NUDT15 depletion[29](Fig. 5f). These data demonstrate that 6-TG potentiation *via* TH1760 is unsurprisingly unrelated to the MMR machinery and more importantly, that NUDT15 inhibition is a potentially viable path to re-sensitize 6-TG-resistant malignancies. This is further supported by the observation that TH1760 effectively reduced 6-TG cytotoxic IC_{50} values by 10-fold in 697 cells, a B-ALL cell line harboring a hyperactive variant (R238W)[36] of the nucleotidase NT5C2 (Extended Data 4f), another resistance-driving mutation exhibited among relapsed ALL patients[37]. Additionally, using a pair of isogenic fibroblast cell lines with vastly different malignant potentials, i.e., the hTERT-immortalized BJ-hTERT cells and their tumorigenic progeny BJ-RAS cells that express SV40 large T antigen and oncogenic HRAS[38], we observed that TH1760 preferentially sensitized BJ-RAS cells to 6-TG versus their non-transformed counterpart BJ-hTERT cells (Fig. 5g), further indicating that particularly in the presence of oncogene, TH1760 may confer thiopurine a potential widening of its therapeutic window, which warrants further investigation.

Mechanistically, compounds that increase thiopurine toxicity through inhibiting NUDT15 should also result in elevated accumulation of 6-thio-(d)GTP in nucleic acids. Combining TH1760 with thiopurines significantly elevated the intracellular accumulation of 6-thio-dGTP/6-thio-GTP and their incorporation into DNA/RNA, respectively, determined by the DNA/RNA radioactivity levels upon treatment with ^{14}C-labelled 6-MP (Fig. 6a; Extended Data 5a), or more precisely by identifying the 6-thio-(d)GTP lesions *via* mass spectrometry when treated with label-free 6-TG (Fig. 6b; Extended Data 5b). The intracellular accumulation of 6-thio-(d)GTP further coincided with increases in DNA damage (higher comet tail moment) (Fig. 6c), DNA damage repair responses (induction of γH2AX, CHK1 and CHK2 phosphorylation), G2-phase cell cycle arrest, and finally, apoptosis (induction of cleaved PARP and caspase 3) (Fig. 6d; Extended Data 5c-d), all of which recapitulated thiopurine-induced responses in NUDT15-depleted cells[29]. Altogether, these data strongly suggest that TH1760 is a *bona fide* potent, selective and cell-active probe for NUDT15.

Discussion

The human NUDIX family has proven to be remarkably diverse in both their substrates and functions, following a period of initial characterization as seen through the lens of oxidized

nucleotide sanitation[3]. Genetic and chemical biology-based exploration of their roles has elucidated novel biological functions and influences on disease pathology and treatment[39], and more importantly, underscored the importance of developing small molecule probes that can dissect the functional underpinnings of NUDIX enzymes within a cellular context.

NUDT15 (MTH2) was first described as a sanitizer of the oxidized nucleotide pool akin to and as a potential redundancy factor for MTH1[5–7]; however, more recent evidence has suggested that the contribution of NUDT15 to this process is likely minimal[8]. Following a series of pharmacogenomics reports demonstrating a strong association between NUDT15 missense mutations and thiopurine intolerance in patients, we and others discovered that NUDT15 hydrolyzes the active metabolites of thiopurine treatments thereby limiting their toxicity and explaining why destabilizing missense mutations predispose patients to thiopurine intolerance[16,29]. Nonetheless, thiopurines are not natural substrates and the physiological functions of NUDT15 in human cells are still unknown. In fact, NUDT15 knockout mice show no gross physiological changes or predisposition to poor health[30].

Here, we describe TH1760 as the first specific small molecule inhibitor to probe NUDT15 function(s) in cells. Following conventional high-throughput screening and structure-based design, we comprehensively demonstrated that TH1760 potently inhibits and binds NUDT15 enzymatic function *in vitro* and in cells. At the tested concentration of 10 μM, TH1760 effectively engaged intracellular NUDT15 and further strongly potentiated its substrate thiopurines metabolites, without demonstrating apparent off-target toxicity. We additionally validated TH1760 as a specific NUDT15 probe with an inactive structural analog, TH7285. The addition of a methyl group on the nitrogen of the benzoxazolone ring completely abolished the binding to NUDT15 *in vitro* and in cells, as well as had no effect on thiopurine cytotoxicity, thus confirming that potentiation of thiopurine toxicity is a direct effect of inhibiting NUDT15 enzymatic activity. This is in line with the inability of the catalytically-compromised E67A mutant to hydrolyze NUDT15 substrates or to rescue cells from thiopurine toxicity (Extended Data 3e; Fig. 4c).

While it is clear that catalytic inhibition of NUDT15 potentiates thiopurine efficacy, it is debatable if NUDT15 inhibitors would be of clinical benefit as a thiopurine combination therapy. A recent report using a novel NUDT15 knockout mouse model, demonstrated that NUDT15 can guide thiopurine therapy by balancing the toxicity and anti-leukemic efficacy[30]. They have confirmed that therapeutic efficacy is preserved in Nudt15$^{-/-}$ mice on a reduced 6-MP dose compared to Nudt15$^{+/+}$ counterparts exposed to a standard dosage (20-fold decrease). These results suggest that it is feasible to treat leukemia patients with systemically low NUDT15 activity with a reduced thiopurine dosing regimen, and further indicate an opportunity to employ NUDT15 inhibitors such as TH1760 as an additional measure to fine-tune thiopurine dosing in the clinic. Also on a positive note, we preliminarily observed that TH1760 could preferentially potentiate the tumorigenic versus non-transformed fibroblast cells (Fig. 5g). Still, lack of conclusive evidence of NUDT15 being overexpressed or hyperactivated in disease target cells (e.g., by activating mutations) makes it uncertain if a sufficient therapeutic window exists to justify broadly utilizing NUDT15 inhibitors as a booster for thiopurine-based treatment regimens.

Nevertheless, it has recently been shown that a thiopurine-derived compound, 6-thio-dG, can be readily incorporated into *de novo* synthesized telomere as 6-thio-dGTP, thereby inducing telomere dysfunction and selective cytotoxicity in telomerase-expressing cancer cells such as glioma and medulloblastoma[27,28]. While the studies of 6-thio-dG still remain pre-clinical, it is certainly worthy to explore the therapeutic outcome of combining NUDT15 inhibition, potentially *via* TH1760, to this process.

Interestingly, we saw that while re-expression of wild-type NUDT15 could rescue the effect of NUDT15 depletion on thiopurine toxicity, overexpression in cells with basal NUDT15 activity was unable to appreciably desensitize them, despite a roughly 10-fold increase in overall NUDT15 expression (Extended Data 3f, h). This could suggest that increased NUDT15 activity alone is not sufficient to cause resistance to thiopurine therapies, and likely reflects the combined effects of multiple thiopurine-metabolizing and effector enzymes on toxicity[40–42]. This is further appreciated by the high variability of NUDT15-induced thiopurine sensitization in different hematological cell lines (Fig. 5c, Extended Data 4a,b). Given the complex picture of thiopurine metabolism, nevertheless, using TH1760, we could re-sensitize cell lines harboring clinically relevant 6-TG resistance mutations, including B-ALL cell line 697 that expresses a relapse-specific hyperactive mutant (R238W) of the nucleotidase NT5C2[36,37,43], and colorectal carcinoma cell line HCT116 that has defective MMR machinery[24,29] (Fig. 5f, Extended Data 4f). These data clearly suggest that TH1760 is a valuable tool to decipher the potential of NUDT15 inhibition in overcoming emerging resistance during thiopurine therapy[37].

Aside from 6-thio-(d)GTP, NUDT15 has also demonstrated considerable activity against canonical nucleotides such as dGTP, dUTP and dTTP[8], indicating potential catalytic activity against their analogues. Comprehensive biochemical and/or cell-based screening of therapeutically relevant nucleoside/nucleotide analogues will elucidate the role of NUDT15 on their metabolism and efficacies, and additionally if NUDT15 inhibition *via* TH1760 could improve their therapeutic efficacies.

Perhaps more importantly, the availability of a chemical probe to rapidly control NUDT15 catalytic activity should prove invaluable to understanding its underlying biological functions, as well as additional contexts for therapeutic intervention. Approaches with expression ablation of NUDT15 (siRNA, shRNA), while consistently showing negligible effects on cellular fitness or proliferation capacity (Extended Data 3c-d), do not possess the temporal precision or the differentiation between the enzymatic versus non-enzymatic functions, which can be instead provided by a cell-active inhibitor. For these reasons, we herein present TH1760, the first *bona fide* highly potent and selective NUDT15 inhibitor to interrogate NUDT15 biology and furthermore, as a tool to uncover novel treatment options against human diseases.

Online Methods

Protein production

WT NUDT15, MTH1, NUDT2, NUDT5, NUDT9, NUDT12, NUDT14, NUDT18, dCTPase, ITPase, dUTPase and NUDT22 were expressed and purified as before (see

Supplementary Fig. 6 for enzyme purity)[8,39,44]. NUDT15 E67A was generated using site-directed mutagenesis using Phusion High-Fidelity PCR Master Mix (Thermo Fisher Scientific), an annealing temperature of 55 °C and the following oligonucleotides:

NUDT15E67A_F:	5' – GGGAAACCTGGGAAGCAGCAGCTCTTCACC – 3'
NUDT15E67A_R:	5' – GGTGAAGAGCTGCTGCTTCCCAGGTTTCCC – 3'

Sequence-verified NUDT15 E67A construct was then expressed from pNIC28 (Novagen) in E. coli Rosetta (Novagen) upon induction by 0.5 mM IPTG, followed by bacteria lysis using BugBuster protein extraction reagent (Millipore) supplemented with benzonase (2.5 U/mL, Merck-Millipore) and cOmplete Mini, EDTA-free protease inhibitor (Roche). Protein was purified from clarified lysates on a HisTrap column (GE Healthcare), using buffer A (20 mM HEPES pH 7.5, 250 mM NaCl, 25 mM Imidazole) as starting buffer and an imidazole gradient (25–500 mM) in buffer A as the elution buffer. Protein-containing fractions were confirmed by SDS-PAGE and pooled for dialysis in 20 mM HEPES pH 7.5, 20 mM NaCl, 10% glycerol. NUDT15 E67A was further purified on a MonoQ column (GE Healthcare) using Buffer B (20 mM HEPES pH 7.5, 20 mM NaCl, 10% glycerol) and eluted using a gradient of NaCl in buffer B ranging from 0.02-1.0 M NaCl. Protein-containing fractions were confirmed by SDS-PAGE and His-tag was removed by TEV protease, followed by purifying the reaction mixture with a His Trap column as described. Flow through was dialyzed overnight in storage buffer (20 mM HEPES pH 7.5, 300 mM NaCl, 10% glycerol, 1 mM TCEP), aliquoted and stored at 80°C. All purification was performed in the absence of reducing agent.

Protein purities were confirmed using SDS-PAGE and Coomassie staining, and concentrations were determined by NanoDrop (Thermo Fisher Scientific) A280 measurement.

In vitro NUDT15 activity assay

Malachite green assay—NUDT15 enzymatic activity and *in vitro* potency evaluation of putative NUDT15 inhibitor were determined using a previously described enzyme-couple malachite green assay[8]. Briefly, 2nM recombinant NUDT15 in reaction buffer (100 mM Tris-Acetate pH 8.0, 40 mM NaCl, 10 mM Mg-Acetate, 1 mM DTT) was incubated with 50 μM dGTP (Sigma Aldrich D4010), alone or with test compounds at desired concentrations, at 22°C for 20 min. Buffer only served as positive control for complete enzyme inhibition. Hydrolysis reaction was then coupled to an excess of *E. coli* pyrophosphatase (0.4 U/mL, Sigma-Aldrich I5907) for 20 min under agitation to convert hydrolysis-released pyrophosphate (PPi) to inorganic phosphate, which was in turn measured by absorbance at 630 nm after incubating with malachite green reagent for 15 min under agitation. The catalytic activity of NUDT15 E67A mutant against 6-thio-dGTP was similarly determined, with exception of using 50 μM 6-Thio-dGTP as reaction substrate, and the inclusion of a PPi standard curve ranging from 0 to 5 μM PPi to calculate produced PPi.

PPiLight inorganic pyrophosphate assay—Inhibition of the 6-thiodGTPase activity was performed using PPiLight inorganic pyrophosphate assay (Lonza, #LT07-610), where assay pH is close to cellular conditions. Briefly, inhibition curves were produced for TH1760 using a dilution series ranging from 13.3 μM to 75 pM, for TH884 and TH7285 from 15 μM to 2.2 nM. Activity of 10 nM NUDT15 activity was determined in assay buffer (100 mM Tris acetate pH 7.5, 40 mM NaCl, 100 mM Magnesium acetate, 1 mM DTT). Since the Km of NUDT15 for 6-thio-dGTP was previously determined to 2 μM[29], a 6-thio-dGTP (Jena Bioscience, NU-1213S) concentration of 2.5 μM was used in the assay. The reaction mixture was incubated by shaking at 22 °C for 30 minutes before detection of formed PPi using PPiLight inorganic pyrophosphate assay (Lonza, #LT07-610) via luminescence reading in a Hidex plate reader.

Small molecule library composition

The screen for NUDT15 inhibitors was conducted at the Chemical Biology Consortium Sweden (www.cbcs.se). The screening campaign comprised a combination of in-house and commercially available libraries, amounting to a total of 17,946 compounds. The commercial compounds originate from Enamine, whereas the in-house libraries were partly donated by Biovitrum AB, Sweden (the origin and composition has been described previously)[31]. Compounds included in the screening set were selected to represent a diverse selection of a larger set of 65,000 compounds, while keeping a certain depth to allow crude structure–activity relationship studies. The selection was also biased towards lead-like and drug-like profiles with regards to molecular weight, hydrogen bond donors/acceptors and LogP1.

For long-term storage the compounds are kept frozen at -20°C as 10 mM solutions in dimethyl sulfoxide (DMSO) under low humidity conditions in REMP 96 Storage Tube Racks in a REMP Small-Size Store™. To facilitate screening aliquots of the stock solutions were transferred to Labcyte 384 LDV plates (LP-0200) and then further into Labcyte 1536 HighBase plates (LP-03730) to enable dispensing using an Echo 550™ acoustic liquid handler (LabCyte). For this campaign 40 nL of the compound solutions were dispensed directly into columns 1-22 of the 384-well assay plates (Nunc 242757), while columns 23 and 24 were reserved for controls as outlined below. The plates were sealed with a peelable Aluminum seal (Agilent 24210-001) using a PlateLoc thermal microplate sealer (Agilent) and kept at RT until used. The final compound concentration in the screen was 10 μM with a final DMSO concentration of 0.1% in all wells.

Small molecule NUDT15 inhibitor screening campaign

Screening of small molecule NUDT15 inhibitors were conducted using the enzyme-coupled malachite green assay. Recombinant human NUDT15 (2nM) was incubated with 50 μM dGTP, alone or in combination with screening compounds (100 μM), in the assay buffer (10 mM Tris-Acetate at pH 8.0, 40 mM sodium chloride, 10 mM magnesium acetate, 0.005% Tween-20 and 1 mM dithiothreitol) at RT for 1 h. The hydrolysis reaction was then coupled to a significant excess of inorganic pyrophosphatase (0.4 U/mL) to convert hydrolysis-resulted pyrophosphate to inorganic phosphate, which was in turn measured by absorbance

at 630 nm (read time 0.1 s/well, Victor 3 from PerkinElmer) after incubating with malachite green reagent for a minimum of 8 min under agitation.

Screening assay was conducted with total assay volume of 40 μL/well in 384-well assay plates (Nunc 242757), composed of 10 μL enzyme solution, 30 μL substrate solution and 40 nl 10mM compounds solutions pre-dispensed using a FlexDrop IV (PerkinElmer). On each assay plate, column 24 contained NUDT15-free reaction buffer only and served as positive control (100% enzyme inhibition), while column 23 without compound served as negative control (0% inhibition). Raw absorbance value at 630 nm was then normalized to negative and positive controls on each individual plate. Hit-limit was identified by the average plus three standard deviations of the library compound responses, resulting in a hit rate of 0.55%. Subsequent three-dose (2.5, 10 and 20 μM) hit confirmation was conducted using the same assay condition.

Selectivity assay for TH1760

The selectivity assay for TH1760 against pyrophosphatase and/or other NUDIX enzymes were conducted using MTH1, NUDT2, NUDT5, NUDT9, NUDT12, NUDT 14, NUDT18, NUDT22, ITPase, dCTPase and dUTPase, as described previously[8,39,44,45]. Briefly, enzyme activities were determined using enzyme-coupled malachite green assays, where individual enzymes were incubated with desired substrate alone or in combination with 100 μM TH1760, for 15-20 min at room temperature (RT) in the reaction buffer (100 mM Tris Acetate, pH 8, 40 mM NaCl, 10 mM MgAc, 1 mM DTT, 0.005% Tween 20). Coupled enzymes and malachite green reagent were subsequently added to allow the measurement of reaction-released inorganic phosphate *via* absorbance at 630 nm. Specific assay conditions are summarized in Supplementary Fig. 7.

Crystallization and structure determination

Full length NUDT15 (20 mg/mL) was crystallized in the presence of α-Chymotrypsin (0.2 mg/mL) and 10 mM of TH1760 dissolved in DMSO 20 mM HEPES, pH 7.5, 300 mM NaCl, 10% Glycerol and 1 mM TCEP. Sitting drop vapor diffusion experiments at 18°C were performed, and NUDT15 was mixed with reservoir solution (0.1 M Tris-HCl pH 8.5, 0.15 M MgCl2, and 30% PEG3350) in a 1:2 ratio. Diffraction quality crystals appeared in the first week, followed by quick extraction without additional cryoprotectant and flash frozen in liquid nitrogen. Data collection was performed at 100 K and a wavelength of 0.9 Å, at beam line 14.1 (BESSY, Germany). Data reduction and processing were carried out using iMOSFLM[46] and Aimless[47] from the CCP4 suite[48]. The structure was solved by molecular replacement of the template structure file with PDB ID 5LPG using Phaser [49] followed by iterative building cycles using the Refine program in Phenix[50]. TLS parameters were determined using the TLSMD webserver[51]. Relevant statistics can be found in the Supplementary Table 4. The NUDT15-TH1760 co-crystal structure was deposited in the protein database (PDB), ID 6T5J.

Cell culture

NB4, HL-60, MV4-11, THP-1, PL-21, CCRF-SB, K562, Raji, su-DHL-5, and Wil2-NS cells were cultured in RPMI medium with GlutaMAX; U2OS, BJ-hTERT, and BJ-RAS cells in

DMEM medium; 697 cells in RPMI medium with 250 mM HEPES buffer; HCT116 and HCT116 3-6 in McCoy's 5A (Modified) Medium; and HEK293T cells in Dulbecco's Modified Eagle Medium at 37 °C with 5% CO2 in a humidified incubator. All culture medium were purchased from ThermoFisher Scientific and supplemented with 10% heat-inactivated fetal bovine serum (FBS) and penicillin/streptomycin (100 U/mL and 100μg/mL, respectively). All the cell lines were obtained from ATCC, with the exceptions of PL-21 (gifted by Dr. Sören Lehmann, Karolinska Institutet, Sweden), HCT116 and HCT116 3-6 (gifted by Dr. Bert Vogelstein, Johns Hopkins), 697 (gifted by Dr. Magnus Bjorkholm, Karolinska Institutet, Sweden) and BJ fibroblasts (gifted by Dr. William C. Hahn, Dana Faber Cancer Institute). All cell lines were regularly monitored and tested negative for the presence of mycoplasma using a commercial biochemical test (MycoAlert, Lonza).

Drugs and Antibodies

Doxycycline hydrochloride (Sigma-Aldrich) was dissolved in MilliQ water. Thiopurines, 6-thioguanine (Sigma-Aldrich) and mercaptopurine (Merck AG), and all NUDT15 inhibitors were dissolved in DMSO to a stock of 10 mM. Antibodies against phosphorylated Chk1 (rabbit, Ser345; cat. no. 2348), Chk1 (mouse, cat. no. 2360), phosphorylated Chk2 (rabbit, Thr68; cat. no. 2197), Chk2 (mouse, cat. no. 3440), phospho-Histone H2A.X (rabbit, Ser139; cat. no. 2577), cleaved PARP (rabbit, cat. no. 9541), HA-tag (mouse, cat. no. 2367) and cleaved caspase 3 (rabbit, cat. no. 9661) were purchased from Cell Signaling Technology. Antibodies against NUDT15 (rabbit, cat. no. sc-84533), SOD1 (rabbit, FL-154; cat. no. sc-11407), phosphorylated CDK (rabbit, Thr14/Tyr15; cat. no. sc-28435-R) and Goat anti-mouse IgG-HRP secondary antibody (cat. no. sc-2055) were purchased from Santa Cruz Biotechnology, Inc.. Antibodies against GAPDH (rabbit, cat. no. ab9485) and β-Actin (mouse, cat. no. ab6276) were purchased from Abcam. Donkey anti-mouse IgG IRDye 680RD (cat. no. 925–68072) and goat anti-rabbit IgG IRDye 800CW (cat. no. 925–32211) were purchased from Li-Cor.

Target engagement assays

Differential Scanning Fluorimetry (DSF)—NUDT15 DSF was performed as described before[29]. Briefly, recombinant NUDT15 protein (4μM), Sypro Orange (5X, Thermo Fischer Scientific), and DMSO or putative NUDT15 inhibitors were combined in assay buffer (100 mM Tris Acetate, pH 8, 40 mM NaCl, 10 mM MgAc) in 96-well PCR plates at the final volume of 20 μL/well and DMSO concentration of 2%. The assay mixture was then subject to a 25-95 °C temperature gradient (1°C/min increments) with fluorescence intensities measured every minute, on a CFX96 Real-Time PCR machine (Bio-Rad). Melting temperatures were determined by curve-fitting fluorescence intensity using Boltzmann sigmoidal non-linear fitting (GraphPad Prism).

Drug affinity responsive target stability (DARTS)—DARTS was performed based on the previously described method[34]. Compounds were applied at indicated concentrations to HCT116 or U2OS cells for 1-4 h, before or after, respectively, cell lysis using M-PER™ Mammalian Protein Extraction Reagent (Thermo Fisher) supplemented with cOmplete Mini protease inhibitor. Cell lysates were then subject to pronase digestion in TN buffer (50 mM Tris-HCl, pH 8.0; 50 mM NaCl) at the protein-to-pronase ratio of 25:1 for U2OS lysate and

Europe PMC Funders Author Manuscripts

100-400:1 for HCT116 lysate, for 30 min at RT. For the non-digested (ND) samples, TN buffer was added instead of pronase. Samples were then prepared for Western blot to detect NUDT15 in U2OS cells or HA-tagged NUDT15 in HCT116. GAPDH served as the loading control.

Cellular thermal shift assay (CETSA)—CETSA was performed with intact cells as described previously[39,52]. Briefly, NB4 or HL-60 cells overexpressing pInducer20-3xHA-NUDT15 WT were induced with 1 μg/mL doxycycline overnight. For CETSA, cells were incubated with DMSO (0.3% v/v), 30 μM TH884, 30 μM TH7285, 10 μM TH1760 or 30 μM TH1760. For iso-thermal dose response fingerprint (ITDRF) CETSA, cells were subdivided and treated with the indicated concentrations of TH1760 (with equivalent final DMSO v/v). Three hours post-treatment at 37°C and 5% CO_2 in a humidified incubator, the cells were harvested, washed twice in PBS to remove excess compound, and then resuspended in TBS supplemented with cOmplete™, Mini, EDTA-free Protease Inhibitor Cocktail (Roche, Merck) at $1.0x10^6$ cells per 60 μL. Following heating at the indicated temperature (CETSA) or 53°C (ITDRF CETSA) for 3 minutes in Veriti 96-well Thermal Cycler (ABI), the samples were equilibrated at room temperature for an additional 3 minutes prior to lysing by 3x freeze-thaw cycles with an ethanol-dry ice and 37°C water bath. The lysates were then clarified by centrifugation at 20,000 x g for 20 minutes at 4°C and prepared for western blotting to detect HA-tagged NUDT15. SOD-1 served as the loading control.

Western blotting

Cells with indicated treatment were washed with ice-cold PBS, collected in lysis buffer (50 mM Tris (pH 8.0), 150 mM sodium chloride, 1.0% NP-40, 0.5% sodium deoxycholate, 0.1% sodium dodecyl sulphate, 1X cOmplete™ EDTA-free protease inhibitor, and 1X Phosphatase Inhibitor cocktail (Life Technologies)), and sonicated using the UP100H ultrasonic processor (Hielscher). Upon clarification *via* centrifugation, lysates containing 20-30 μg total protein (measured using Pierce™ BCA Protein Assay Kit, Thermo Fisher) were mixed with β-mercaptoethanol-supplemented 4x Laemmli buffer (Bio-Rad) before being heated at 95°C for 5-10 min. Proteins were then separated by SDS-PAGE with 4–15% Mini-PROTEAN TGX gels, and transferred to a nitrocellulose membrane with a Trans-Blot Turbo machine (Bio-Rad). Membranes were blocked with Odyssey Blocking Buffer (LI-COR), and probed with primary antibodies against desired target protein at 4°C overnight and then with species-appropriate secondary antibodies at RT for 30 min. Membranes were washed three times with TBST between incubations. Protein bands were visualized with an Odyssey Fc Imager, directly when using fluorescence-conjugated secondary antibodies (Li-Cor) or upon adding Clarity Western ECL substrate (Bio-Rad) when using HRP-conjugated antibody. Images were analyzed using Image Studio Software (Li-Cor Biosciences), and all uncropped images are provided in Source Data.

Cloning of mammalian lentiviral constructs

NUDT15-specific (TRCN0000050311, shN15) or non-targeting (shNT) shRNA lentiviral constructs were generated using the Tet-pLKO.1-puro lentiviral vector (gifted by Dmitri

Wiederschain; Addgene plasmid #21915) as described previously[29]. The pInducer20-3xHA-NUDT15 lentiviral constructs non-resistant to shN15 were generated as described[29].

The shN15-resistant NUDT15 overexpression vectors (WT, E67A and R139C) were constructed by firstly cloning WT, E67A, or R139 NUDT15 sequences into pENTR4-N-3xHA, as reported previously[29]. To create resistance to shN15 shRNA, site-directed mutagenesis was utilized with the following primers to insert silent mutations at every third base:

F1:	5’ – phospho - CTA CAT CTA AAG AAT GTT CAC TTT GCC TCA GTT G – 3’
R1:	5’ – phospho - CGC AGC CTC TTC CCA GGT TTC CCT TTG – 3’
R2 (E67A):	5’ – phospho - CGC AGC CGC TTC CCA GGT TTC CCT TTG – 3’

Following PCR amplification with Phusion polymerase (ThermoFisher Scientific), PCR products were confirmed by gel electrophoresis and digested with DpnI (ThermoFisher Scientific) to enrich for mutagenized NUDT15 plasmid. Sequence verified clones were then shuttled into the pInducer20 lentiviral construct (gifted by Stephen Elledge; Addgene plasmid #44012) using Gateway® LR Clonase® II Enzyme mix.

Lentiviral transfection

Lentiviral vectors were produced by transfecting HEK293T cells with lentiviral plasmids using calcium phosphate precipitation method as described before[29]. Selection for stable transductants was achieved using 1 μg/mL puromycin (Sigma-Aldrich; Tet-pLKO.1-puro, EF1α-ORF-mPGK-puro, lentiCRISPRv2_scr) and/or 400 μg/mL neomycin (G418, Sigma Aldrich; pInducer20).

Cell viability assays

Cells were seeded in 96-well or 384-well assay plates at 50000 cells/mL and treated with indicated concentrations of thiopurines, alone or subsequent to 3 h treatment with putative NUDT15 inhibitor. Four days post-treatment, resazurin sodium salt (10 μg/mL) was added, and cell viabilities were assessed by measuring fluorescence intensity at 544/590 nm (Ex/Em) upon 2-6 h incubation with resazurin[53], using a HidexSense plate reader (Hidex). Cells stably expressing doxycycline-inducible constructs were pre-treated with doxycycline for 48 h prior to seeding. Medium only and cell only wells served as negative and positive controls, respectively. Relative cell viabilities were calculated by subtracting the averaged negative control fluorescence signals and then normalizing to the positive control signals, which were then used to determine compound EC_{50} values *via* nonlinear curve fitting with variable slope (four parameters) in GraphPad Prism Software Inc.. The relative viabilities were further compiled into a data frame to calculate drug combination synergy scores using SynergyFinder (https://synergyfinder.fimm.fi/)[54].

Flow cytometry analysis

Cells were collected upon indicated treatment, washed with ice-cold PBS, and incubated in staining buffer (50 μg/mL propidium iodide, 20 mM Tris-HCl pH 8.0, 100 mM NaCl, 0.1 % NP40, and 20 μg/mL RNAse) at 4 °C for 1 h, before PI intensity being assessed by Navios flow cytometer (Beckman Coulter) *via* FL3 channel (620/30 nm).

For EdU staining, Cells with indicated treatments were labeled with 10 μM EdU in culture medium at 37 °C for 30 min, before being collected and washed with ice-cold PBS. Cells were then fixed in 0.4% paraformaldehyde at RT for 15 min, permeabilized in 0.1% saponin/1%BSA/PBS over ice for 30 min, and labeled using Click-iT chemistry reagents (4 mM $CuSO_4$, 6 μM ATTO 488 azide, 10 mM ascorbic acid, in PBS) against EdU at RT for 30 min. Signals of ATTO 488 labeled EdU were assessed by Navios flow cytometer (Beckman Coulter) *via* FL1 channel (525/40 nm). Debris-free population was gated out based on forward and side scatter, from which singlets were gated. The G1, S, G2/M, and subG1 population were then gated from the debris-free, singlet population based on PI intensity. The EdU positive population was then gated from the debris-free, singlet population. A total of $4x10^4$ events were acquired per condition per experiment.

Clonogenic survival assay

Clonogenic survival assay was performed as previously described[29]. Briefly, cells were seeded at 200 cells/well in 6-well plates and treated with 6-TG alone or in combination with 10 μM TH1760 for 10 days, before cell colonies were fixed and stained in 4g/L methylene blue/methanol solution. Colonies were subsequently counted and survival fractions were calculated by normalizing the colony numbers to untreated controls.

Measurements of radioactive 6-MP in DNA and RNA

HL-60 cells ($0.5*10^6$) were pre-treated with DMSO or 10 μM TH1760 for 1 h, before 8-^{14}C labelled 6-MP (Moravek Inc.) was added to the cell culture at indicated concentrations. Eighteen hours post-treatment, cellular DNA and RNA were extracted using the E.Z.N.A.® Tissue DNA Kit (Omega) or the Direct-zol RNA miniprep kit (Zymo research), respectively. Samples were then mixed with OptiPhase Supermix Cocktail (Perkin Elmer), followed by radioactivity level measured using a 1450 MicroBeta TriLux.

Mass Spectrometry-assisted measurement of 6-thio-(d)GTP in DNA and RNA

HL-60 cells were pre-treated with DMSO or 10 μM TH1760 for 1 h, before label-free 6-TG was added to the cell culture at indicated concentrations. Eighteen hours post-treatment, cellular DNA and RNA were extracted as described. DNA samples were then treated with 4 μg RNase A (Sigma-Aldrich) and 0.1 U alkaline phosphatase in 200 μL reaction buffer (10 mM ammonium bicarbonate, pH 7.0, and 10 mM $MgCl_2$) at 37°C for 30 min. Similarly, RNA samples were treated with 0.4 U DNase I (Roche Diagnostics) and 0.1 U alkaline phosphatase (Sigma-Aldrich) in 100 μL reaction buffer (40 mM of Tris-HCl, pH 7.9, 10 mM NaCl, 6 mM $MgCl_2$, and 10 mM $CaCl_2$) at 37°C for 30 min. DNA and RNA samples were then precipitated with 0.3 volumes 10 M ammonium acetate and 1 volume isopropanol, washed twice with 70 % ethanol, and re-dissolved in water. Next, samples were hydrolyzed and dephosphorylated to single nucleosides by treatment with 0.1 U Nuclease P1 (Sigma-

Aldrich), 50 U Benzonase nuclease (Santa Cruz Biotechnology), and 0.1 U alkaline phosphatase in 25 μL reactions containing 10 mM ammonium acetate (pH 5.5), 1 mM $MgCl_2$ and 1 mM $ZnCl_2$ for 1 h at 37°C. Directly after hydrolysis, nucleosides were analyzed by high performance liquid chromatography coupled to electrospray ionization mass spectrometry (LC-MS/MS). Thionucleosides were analyzed on a LC-20AS HPLC System (Shimadzu Corporation, Kyoto, Japan) coupled to, an API 5000 triple quadrupole mass spectrometer (AB SCIEX, Farmingham, MA, USA) for DNA thionucleosides and a Triple Quad 5500 mass spectrometer (AB SCIEX) for RNA thionucleosides, both in positive ionization multiple reaction monitoring mode. Chromatography for DNA thionucleoside analysis was performed at 30°C with a Primesep200 mixed-mode column (2.1 mm x 150 mm, 5 μm particle size; SieLC, Prospect Heights, IL, USA) using water and acetonitrile containing 0.1% formic acid as the mobile phase. The following HPLC method was used with a flow rate of 300 μL/min: 5% acetonitrile for 30 s, ramp to 70% by 3 min, hold 70% until 5 min, and return to 5% by 5.1 min until 15 min. Chromatography for RNA thionucleoside analysis was performed at 40°C with a Coresep100 mixed-mode column (2.1 mm x 150 mm, 2.7 μm particle size; SieLC) using water and acetonitrile containing 0.1% formic acid as the mobile phase. The following HPLC method was used with a flow rate of 400 μL/min: 10% acetonitrile for 30 s, ramp to 50% by 2.2 min, hold 50% until 4.4 min, and return to 10% by 4.5 min until 15 min. The canonical DNA and RNA nucleosides were analyzed using the same HPLC column and instrument, but with an isocratic HPLC method using 40% acetonitrile and 0.1% formic acid in water with a flow rate of 500 μL/min for 3 min. Prior to injection, samples were diluted 1:5000 and 1:10 000 in water to analyze canonical nucleosides from DNA and RNA, respectively. The mass transitions were 252.1 → 136.1 for deoxyadenosine, 228.1 → 112.0 for deoxycytidine, 268.1 → 152.0 for deoxyguanosine, 243.1 → 127.0 for thymidine, 268.0 → 136.0 for adenosine, 244.5 → 112.1 for cytosine, 284.0 → 152.1 for guanosine, and 245.0 → 113.0 for uridine.

Alkaline comet assay

Comet assay was performed as previously described[45]. Briefly, NB4 cells were treated with DMSO or 10 μM TH1760 for 3 h before indicated concentrations of 6-TG was added for another 48 h. Upon harvest by centrifugation, cells were resuspended in PBS at $1*10^6$ cells/mL and then mixed 1:5 with 1.2% low melting point agarose (Sigma-Aldrich) at 37 °C. The mixture was then added onto an agarose (1%)-coated fully frosted slides (Fisherfinest™ Premium Superfrost™ Microscope Slides; Thermo-Fisher Scientific), and a cover slip was placed on the mixture until agarose became solidified. Subsequently, cells were incubated in lysis buffer (10 mM Tris-HCl pH 10.0, 2.5 M NaCl, 0.1 M EDTA, 10% DMSO and 1% Triton X-100) at 4°C overnight, and then denatured in electrophoresis buffer (0.3 N NaOH, 1 mM EDTA) for 30 minutes, before electrophoresis at 300 mA, 25 V for 30 minutes using a Comet Assay tank (Thistle Scientific). Slides were then placed into neutralization buffer (0.4 M Tris-HCl pH 7.5) for 45 minutes, and comets were stained using 1x SYBR® Gold Nucleic Acid Gel Stain (ThermoFisher). Images were acquired with a Zeiss LSM 510 confocal microscope and comets analyzed using the Comet assay IV system. A total of 100 cells were analyzed per slide per sample. Tail moment is calculated as per cent DNA in the tail multiplied by the tail length.

DSF-based selectivity screening of TH1760 against a curated kinase library

The assay was performed as previously described[55]. Briefly, recombinant protein kinase domains, 44 in total, at a concentration of 2 μM were mixed with 12 μM of TH1760 or TH7285, in 10mM HEPES, pH 7.5, and 500mM NaCl. Subsequently, temperature-dependent protein unfolding profiles were measured using a Real-Time PCR Mx3005p machine (Stratagene). Experiments were performed in triplicate.

Real-time quantitative polymerase chain reaction (RT-qPCR)

RT-qPCR was performed as described previously[45] and all kits were used according to manufacturer's instructions. Briefly, RNA was isolated from cells using the Direct-zol RNA miniprep kit (Zymo research). 500 ng of RNA was reverse transcribed using the Maxima First Strand cDNA Synthesis Kit for RT-qPCR (Thermo Scientific). RT-qPCR was performed using the Thermo Scientific Luminaris Color HiGreen qPCR Master Mix and the following primers:

β-Actin F:	5'–CCTGGCACCCAGCACAAT–3'
β-Actin R:	5'–GGGCCGGACTCGTCATACT–3'
NUDT15 F:	5'–TGTTCACTTTGCCTCAGTTGTG–3'
NUDT15 R:	5'–AGGAACCCACTCCCAACTTTC–3'

Extended Data

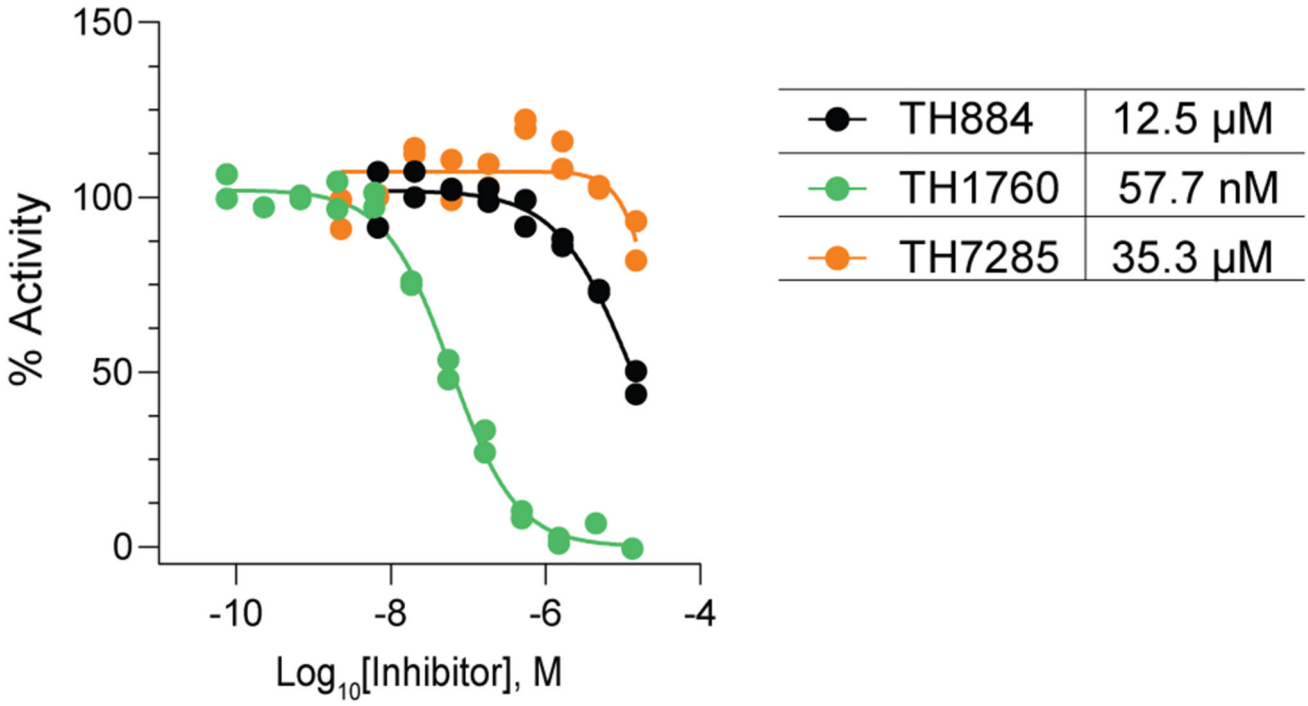

Extended Data Fig. 1. TH1760 potently inhibited the 6-thio-dGTPae activity of NUDT15

TH1760 had over 200-fold potency improvement as compared to TH884, shown using PPiLight inorganic pyrophosphate assay (Lonza, #LT07-610). Individual data of n=2 independent experiments performed in duplicates shown with estimated IC_{50} values.

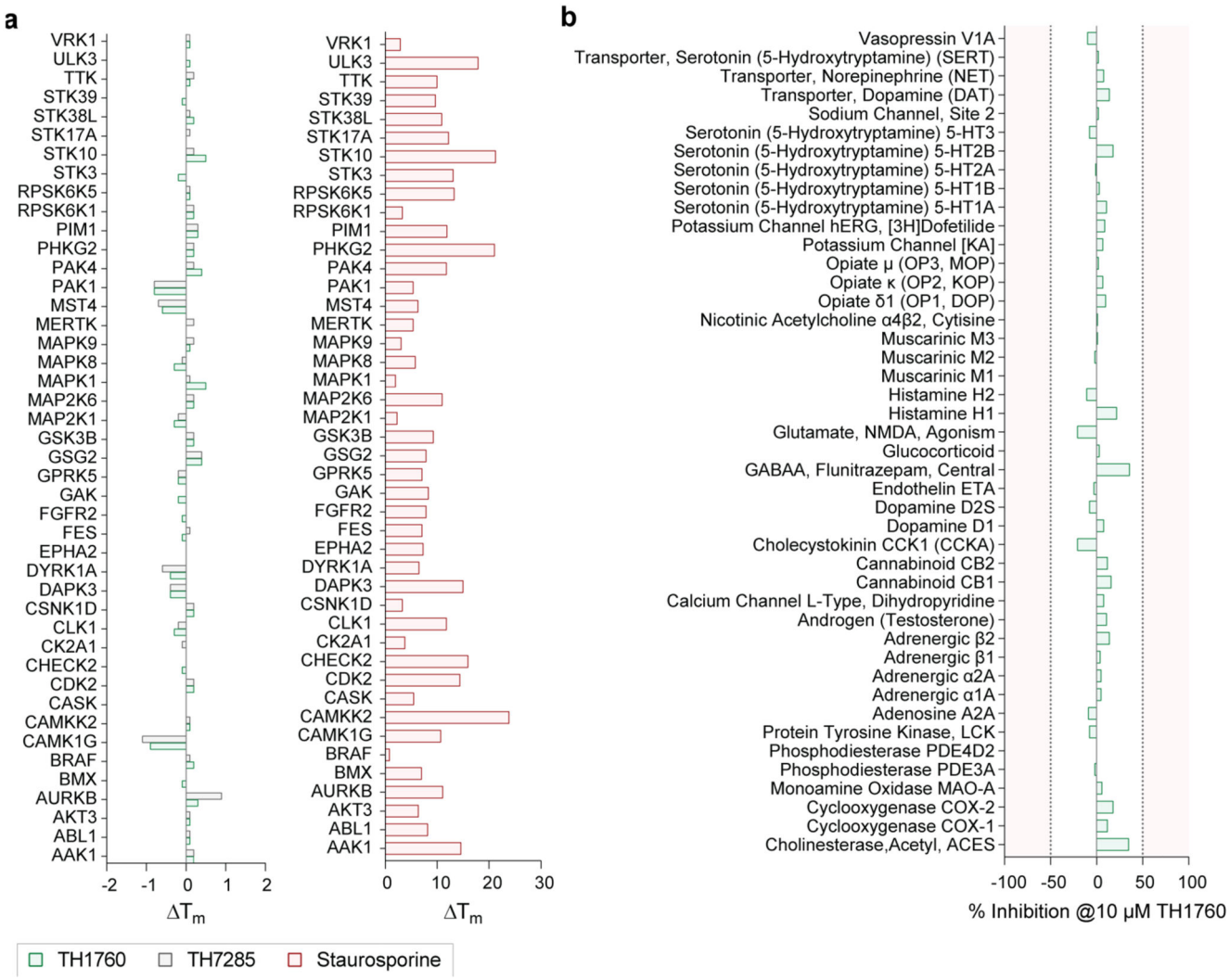

Extended Data Fig. 2. TH1760 demonstrated impressive selectivity

a. TH1760 and TH7285 selectivity at 12 μM against a curated library of 44 kinases, tested using DSF with staurosporine as the positive control compound. Mean change in protein T_m (ΔT_m) of one experiment performed in triplicates shown. **b**. TH1760 selectivity at 10 μM against the SafetyScreen44™ panel from Eurofins Cerep Panlabs. Mean % inhibition of an experiment performed in duplicates shown.

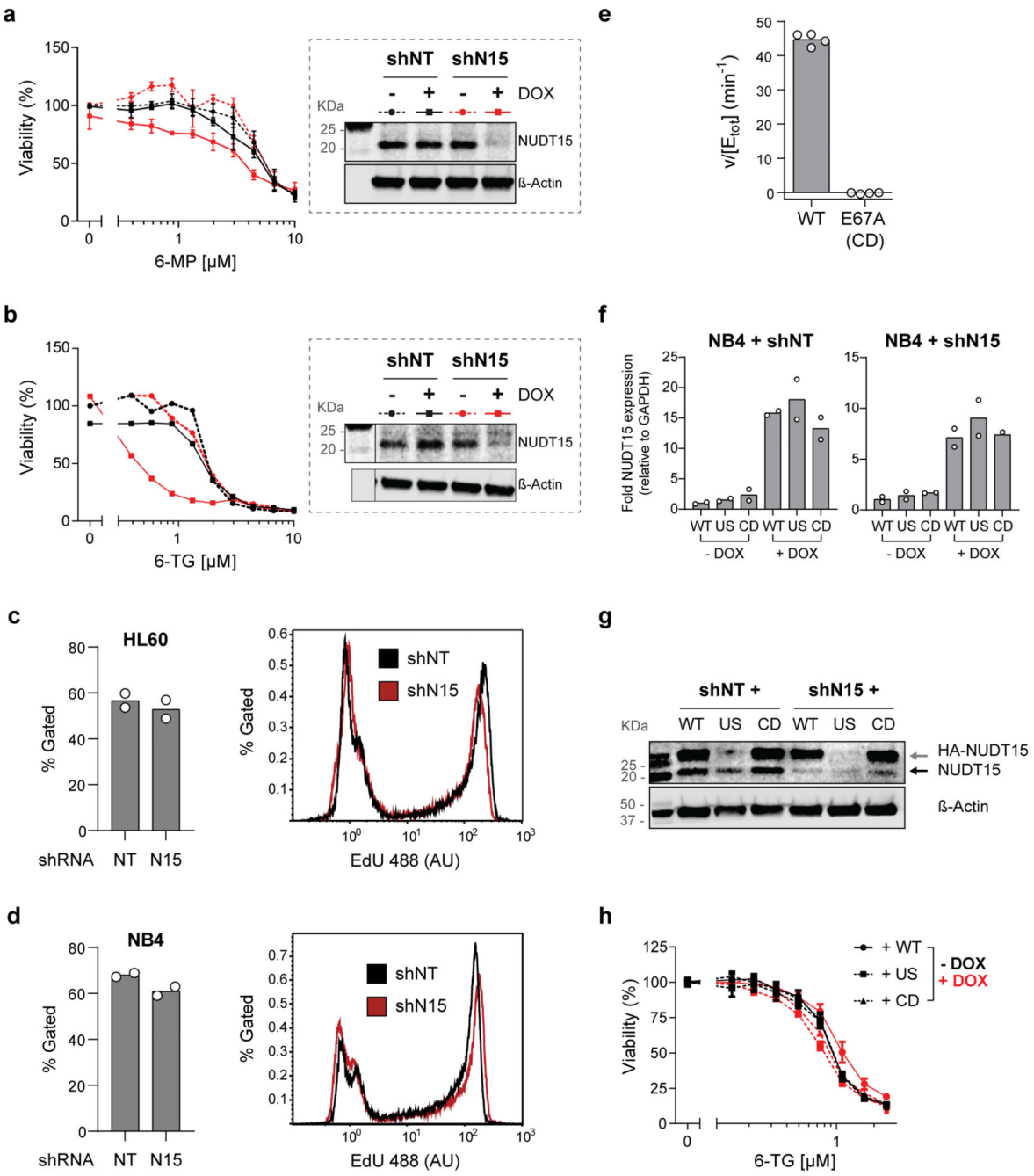

Extended Data Fig. 3. Depletion of NUDT15 in HL-60 and NB4 cells potentiated thiopurine efficacy

a. b. NUDT15 depletion sensitized NB4 cells to 6-MP (a), and HL-60 cells to 6-TG (b). Cell viabilities assessed using resazurin viability assay after 96 (a) or 72 (b) h of treatment and calculated by normalizing to no DOX, DMSO-treated controls. Mean ± SEM of n=3 (a) or mean of n=2 (b)experiments performed in triplicates shown. Left panels: resazurin viability curve; right panels: Western blot demonstrating DOX-induced NUDT15 knockdown. **c**. **d**. Depletion of NUDT15 in HL-60 (c) or NB4 (d) did not affect DNA replication, evidenced by EdU incorporation. Cells expressing DOX-inducible NUDT15-specific (N15) or non-

Europe PMC Funders Author Manuscripts

targeting (NT) shRNA were treated with DOX for 48 h, before EdU labelling. Left panels: Mean EdU+ve population% of n=2 experiments shown. Right panels: representative FACS histogram showing EdU signal intensity. **e**. E67A variant of NUDT15, compared to the wildtype (WT) construct, is catalytically inactive against 6-thio-dGTP (tested at 50μM), shown using enzyme-coupled MG assay. Mean activity of a representative experiment shown with individual repeat values. **f**. RT-qPCR analysis of NUDT15 mRNA levels in NB4 cells co-expressing DOX-inducible shRNA, and shRNA-resistant, HA-tagged NUDT15 constructs (wildtype, WT; unstable, US; or catalytically dead, CD), with GAPHD as the house keeping gene. NUDT15 mRNA levels were normalized to cells expressing WT NUDT15 construct. Mean of n=2 experiments performed in triplicate shown. **g**. Doxycycline treatment induced the co-expression of shRNA (shNT and shN15) and shN15-resistant, HA-tagged NUDT15 overexpression constructs (WT, CD, or US) in NB4 cells. **h**. NB4 cells co-expressing DOX-inducible shNT shRNA and shRNA-resistant, HA-tagged NUDT15 overexpression constructs (WT, CD, or US) were assayed for viabilities under 6-TG treatment. Overexpression of WT NUDT15 conferred marginal resistance to 6-TG Mean ± SEM of n=3 independent experiments performed in duplicates shown.

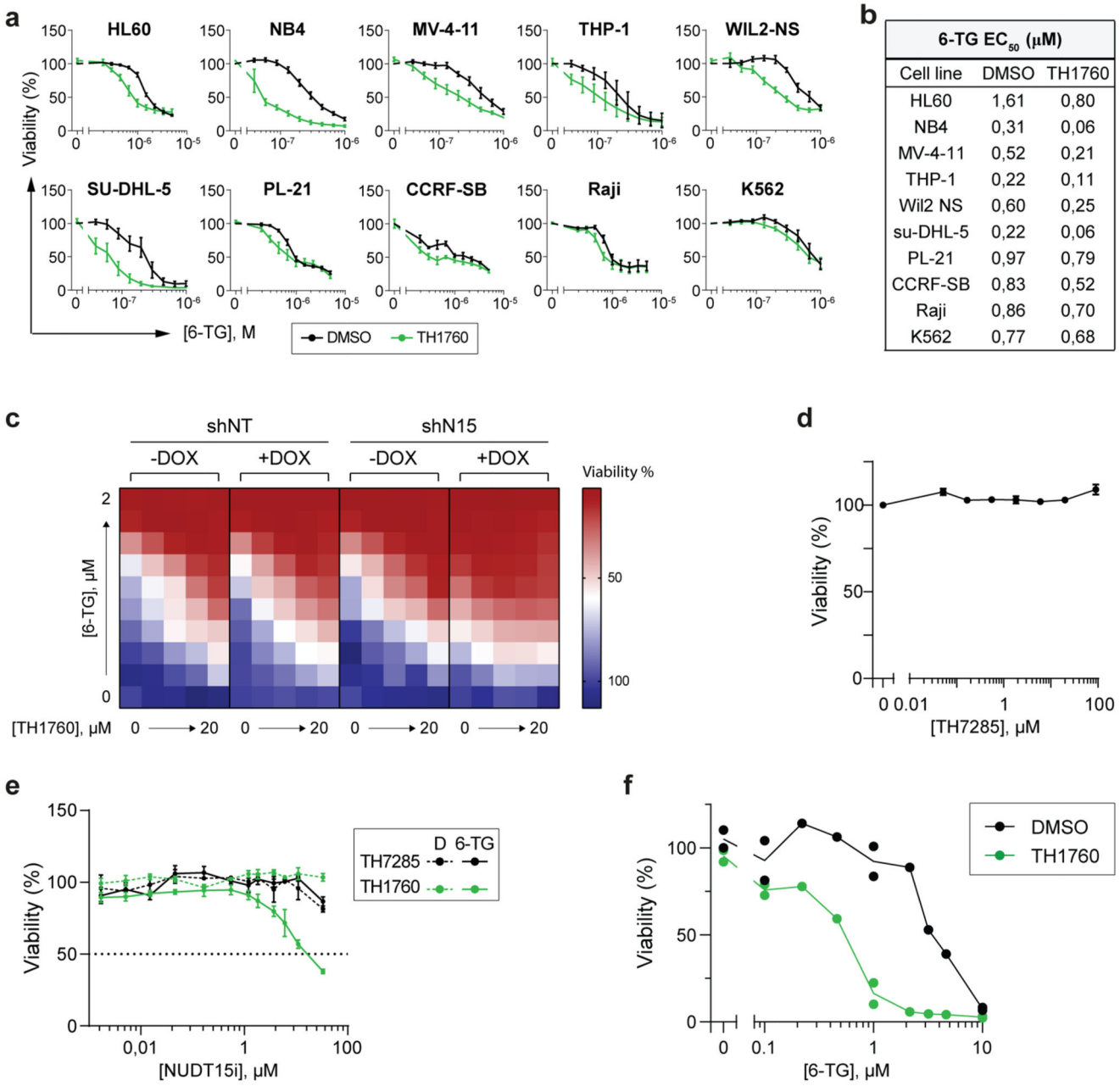

Extended Data Fig. 4. TH1760 treatment sensitized cancer cell lines to thiopurine

a. TH1760 sensitized a panel hematological cell lines to 6-TG. Cells were treated with increasing concentrations of 6-TG alone or in combination with 10 μM TH1760 for 96 h, before viabilities were determined using resazurin viability assay. Viability % was calculated by normalizing to DMSO-treated controls and mean ± SEM of n = 3 experiments shown. **b**. 6-TG cytotoxic EC_{50} values in the cell lines shown in a, determined by curve-fitting cell viabilities *via* non-linear regression model (Graphpad prism, [Inhibitor] vs. response – variable slope model). **c**. TH1760 sensitized NB4 cells to 6-TG in a NUDT15-dependent manner. NB4 cells stably expressing shNT or shN15 shRNA were treated with a dose-

Europe PMC Funders Author Manuscripts

response concentration matrix of 6-TG and TH1760 for 96 h, before viabilities determined by resazurin assay. Viability % was calculated by normalizing to DMSO-treated controls and mean viabilities of n = 2 experiments shown in heat map. **d**. TH7285 was not cytotoxic in HL-60 cells up to 100 μM. Viabilities of HL-60 cells treated with TH7285 for 96h were assessed by resazurin viability assay. Viability % was calculated by normalizing to DMSO-treated controls, and mean ± SEM of n=4 experiments performed in duplicates shown. **e**. TH7285 did not potentiate 6-TG in HL-60 cells. HL-60 cells were treated with 10 μM compounds alone or combined with 320 nM 6-TG (EC_{10}) for 96 h, before resazurin viability assay. Viability % was calculated by normalizing to DMSO-treated controls and mean ± SEM of n = 4 independent experiments shown. **f**. TH1760 (10 μM) substantially reduced the 6-TG EC_{50} in 697 cells by approximately 10-fold, upon co-treatment for 96h. Viabilities determined by resazurin assay and normalized to DMSO-treated control. Viabilities of n=2 experiments performed in duplicates shown.

Europe PMC Funders Author Manuscripts

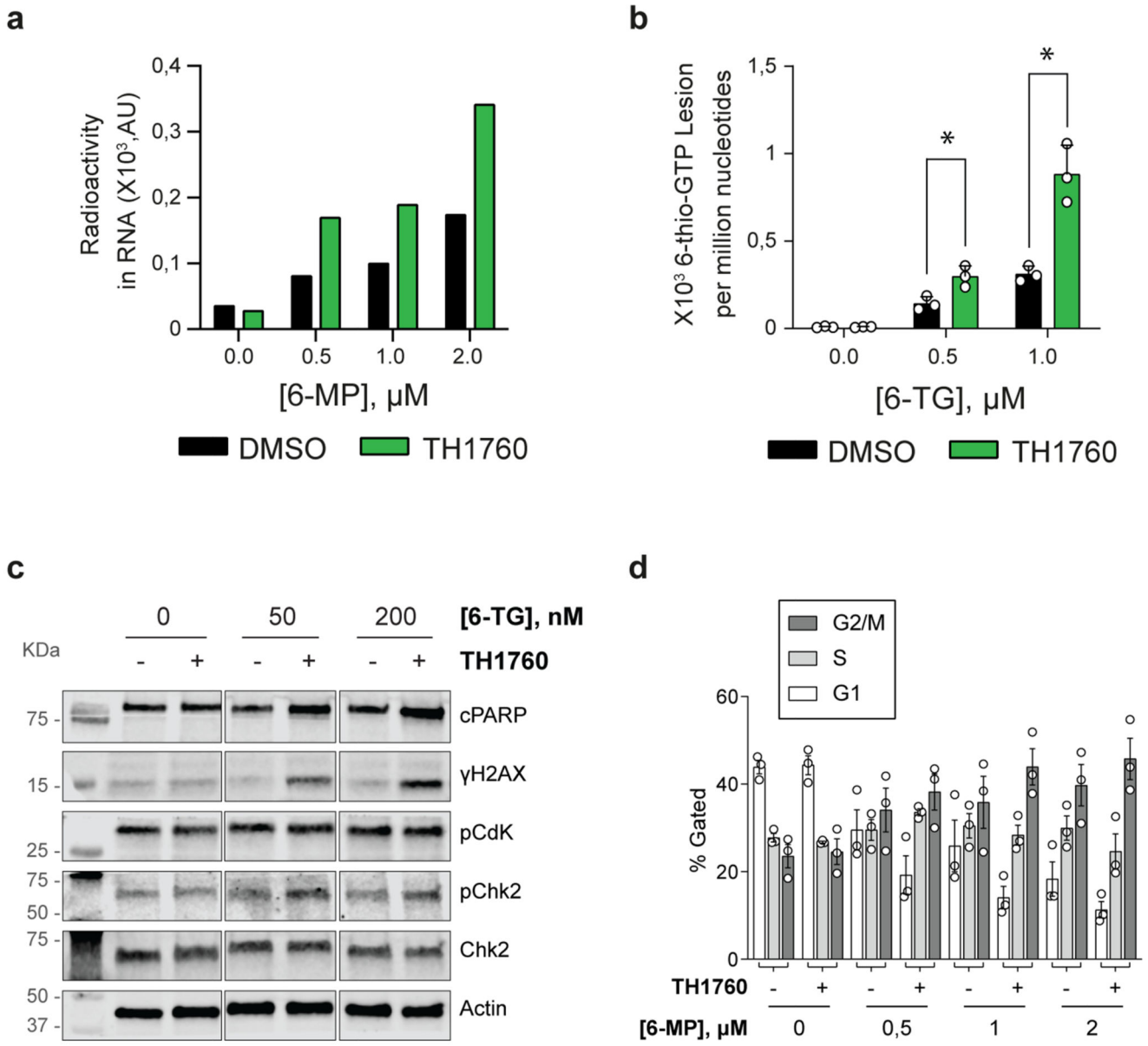

Extended Data Fig. 5. TH1760 potentiated thiopurine-induced cytotoxicity through elevating the intracellular pool of thiopurine metabolites

a. b. TH1760 significantly enhanced the RNA incorporation of metabolites of 6-MP (a) or 6-TG (b). HL-60 cells were treated with increasing concentrations of thiopurines alone or in combination with 10 μM TH1760. Sixteen hours post-treatment, cellular RNA was isolated and incorporation of ^{14}C-labbeled 6-MP metabolites were determined *via* radioactive counts (a) and incorporation of 6-TG metabolites *via* mass spectrometry analysis (b). Mean of n=1 and mean± SEM of n=3 experiment(s) are shown for a and b, respectively. In b, DMSO Vs. TH1760 group: at 0.5μM 6-TG, *p = 0.02, t ratio=3.72, df=4; at 1μM 6-TG, *p = 0.0047, t ratio=5.699, df=4 (two-tailed multiple t-test, Holm-Sidak correction, Graphpad Prism). **c.d**. TH1760 potentiated 6-TG-induced cellular responses in NB4 (c) and HL-60 cells (d). NB4 cells treated with 6-TG alone or in combination with 10 μM TH1760 were assayed for DNA

damage response and apoptotic marker *via* Western blot at 48 h post-treatment. HL-60 cells treated with 6-MP alone or in combination with 10 μM TH1760 were subject to propidium iodide staining followed by cell cycle analysis *via* flow cytometry at 72 h post-treatment. Mean % ± SEM of n=3 independent experiments shown.

Supplementary Material

Refer to Web version on PubMed Central for supplementary material.

Acknowledgments

We thank K. Edfeldt, S. Eriksson, F. Pineiro, L. Sjöholm and A. Thomas for their support in the Helleday Lab. We thank U. Martens and B. Lundgren for compound plating for the biochemical screening campaign. Furthermore, we thank the beamline scientists at BESSY, Germany; Diamond, United Kingdom and the Swiss Light Source, Switzerland for their support in structural biology data collection. Protein production was facilitated by the Protein Science Facility at Karolinska Institutet/SciLifeLab (http://ki.se/psf).

This project was supported by The Knut and Alice Wallenberg Foundation (KAW2014.0273, T.H.; P.S.), the Swedish Research Council (2015-00162, T.H.; 2014-5667, P.S.; 2018-02114, S.G.R), the European Research Council (TAROX-695376, T.H.), Swedish Cancer Society (CAN2015/255, T.H.; 170686, P.S.; 19-0056-JIA, S.G.R.), the Swedish Children's Cancer Foundation (PR2016-0101, T.H.; TJ2017-0021, S.G.R.), the Swedish Pain Relief Foundation (SSF/01-05, T.H.), the Torsten and Ragnar Söderberg Foundation (T.H.), the Canadian Institutes of Health Research and the David and Astrid Hagelén Foundation (B.D.G.P.), the Felix Mindus contribution to Leukemia Research (2019-02004, S.M.Z.), and the EU/EFPIA/OICR/McGill/KTH/Diamond Innovative Medicines Initiative 2 Joint Undertaking (EUbOPEN 875510). SK and AK would like to acknowledge funding by the Frankfurt Cancer Institute (FCI), the German translational cancer consortium site Frankfurt/Mainz (DKTK) and the Structure Genomics Consortium (SGC), a registered charity (number 1097737) that receives funds from AbbVie, Bayer Pharma AG, Boehringer Ingelheim, Canada Foundation for Innovation, Eshelman Institute for Innovation, Genome Canada, Innovative Medicines Initiative (EU/EFPIA, No 875510), Janssen, Merck KGaA Darmstadt Germany, MSD, Novartis Pharma AG, Ontario Ministry of Economic Development and Innovation, Pfizer, São Paulo Research Foundation-FAPESP, Takeda, and Wellcome [106169/ZZ14/Z].

Data Availability Statement

The datasets generated during and/or analyzed during the current study are available from the corresponding author on reasonable request. X-ray NUDT15-TH1760 complex co-crystal structure is deposited in the protein database (PDB), with ID 6T5J.

References

1. Nagy GN, Leveles I, Vertessy BG. Preventive DNA repair by sanitizing the cellular (deoxy)nucleoside triphosphate pool. FEBS J. 2014; 281:4207–23. [PubMed: 25052017]
2. Rudd SG, Valerie NCK, Helleday T. Pathways controlling dNTP pools to maintain genome stability. DNA Repair (Amst). 2016; 44:193–204. [PubMed: 27311542]
3. Bessman MJ, Frick DN, O'Handley SF. The MutT proteins or "Nudix" hydrolases, a family of versatile, widely distributed, "housecleaning" enzymes. J Biol Chem. 1996; 271:25059–62. [PubMed: 8810257]
4. Carreras-Puigvert J, et al. A comprehensive structural, biochemical and biological profiling of the human NUDIX hydrolase family. Nat Commun. 2017; 8:1541. [PubMed: 29142246]
5. Cai JP, Ishibashi T, Takagi Y, Hayakawa H, Sekiguchi M. Mouse MTH2 protein which prevents mutations caused by 8-oxoguanine nucleotides. Biochem Biophys Res Commun. 2003; 305:1073–7. [PubMed: 12767940]
6. Hori M, Satou K, Harashima H, Kamiya H. Suppression of mutagenesis by 8-hydroxy-2′-deoxyguanosine 5′-triphosphate (7,8-dihydro-8-oxo-2′-deoxyguanosine 5′-triphosphate) by human MTH1, MTH2, and NUDT5. Free Radical Biology and Medicine. 2010; 48:1197–1201. [PubMed: 20144704]

Europe PMC Funders Author Manuscripts

7. Takagi Y, et al. Human MTH3 (NUDT18) Protein Hydrolyzes Oxidized Forms of Guanosine and Deoxyguanosine Diphosphates COMPARISON WITH MTH1 AND MTH2. Journal of Biological Chemistry. 2012; 287:21541–21549.
8. Carter M, et al. Crystal structure, biochemical and cellular activities demonstrate separate functions of MTH1 and MTH2. Nat Commun. 2015; 6:7871. [PubMed: 26238318]
9. Song MG, Bail S, Kiledjian M. Multiple Nudix family proteins possess mRNA decapping activity. RNA. 2013; 19:390–9. [PubMed: 23353937]
10. Yu Y, et al. Proliferating Cell Nuclear Antigen Is Protected from Degradation by Forming a Complex with MutT Homolog2. Journal of Biological Chemistry. 2009; 284:19310–19320.
11. Chiengthong K, et al. NUDT15 c.415C>T increases risk of 6-mercaptopurine induced myelosuppression during maintenance therapy in children with acute lymphoblastic leukemia. Haematologica. 2015
12. Yang JJ, et al. Inherited NUDT15 variant is a genetic determinant of mercaptopurine intolerance in children with acute lymphoblastic leukemia. J Clin Oncol. 2015; 33:1235–42. [PubMed: 25624441]
13. Tanaka Y, et al. Susceptibility to 6-MP toxicity conferred by a NUDT15 variant in Japanese children with acute lymphoblastic leukaemia. Br J Haematol. 2015; 171:109–15. [PubMed: 26033531]
14. Yang SK, et al. A common missense variant in NUDT15 confers susceptibility to thiopurine-induced leukopenia. Nat Genet. 2014; 46:1017–20. [PubMed: 25108385]
15. Kakuta Y, et al. NUDT15 R139C causes thiopurine-induced early severe hair loss and leukopenia in Japanese patients with IBD. The Pharmacogenomics Journal. 2015
16. Moriyama T, et al. NUDT15 polymorphisms alter thiopurine metabolism and hematopoietic toxicity. Nat Genet. 2016; 48:367–73. [PubMed: 26878724]
17. Bradford K, Shih DQ. Optimizing 6-mercaptopurine and azathioprine therapy in the management of inflammatory bowel disease. World J Gastroenterol. 2011; 17:4166–73. [PubMed: 22072847]
18. Schmiegelow K, Nielsen SN, Frandsen TL, Nersting J. Mercaptopurine/Methotrexate Maintenance Therapy of Childhood Acute Lymphoblastic Leukemia: Clinical Facts and Fiction. Journal of Pediatric Hematology/Oncology. 2014; 36:503–517. [PubMed: 24936744]
19. Buchner T, et al. Acute myeloid leukaemia (AML): treatment of the older patient. Best Pract Res Clin Haematol. 2001; 14:139–51. [PubMed: 11355928]
20. Shepherd PC, Fooks J, Gray R, Allan NC. Thioguanine used in maintenance therapy of chronic myeloid leukaemia causes non-cirrhotic portal hypertension. Results from MRC CML. II. Trial comparing busulphan with busulphan and thioguanine. Br J Haematol. 1991; 79:185–92. [PubMed: 1958475]
21. Woods WG, et al. Timed-sequential induction therapy improves postremission outcome in acute myeloid leukemia: a report from the Children's Cancer Group. Blood. 1996; 87:4979–89. [PubMed: 8652810]
22. Karran P, Attard N. Thiopurines in current medical practice: molecular mechanisms and contributions to therapy-related cancer. Nat Rev Cancer. 2008; 8:24–36. [PubMed: 18097462]
23. Ling YH, Nelson JA, Cheng YC, Anderson RS, Beattie KL. 2'-Deoxy-6-thioguanosine 5'-triphosphate as a substrate for purified human DNA polymerases and calf thymus terminal deoxynucleotidyltransferase in vitro. Mol Pharmacol. 1991; 40:508–14. [PubMed: 1921985]
24. Swann PF, et al. Role of postreplicative DNA mismatch repair in the cytotoxic action of thioguanine. Science. 1996; 273:1109–11. [PubMed: 8688098]
25. You C, Dai X, Yuan B, Wang Y. Effects of 6-thioguanine and S6-methylthioguanine on transcription in vitro and in human cells. J Biol Chem. 2012; 287:40915–23. [PubMed: 23076150]
26. Yan T, Berry SE, Desai AB, Kinsella TJ. DNA mismatch repair (MMR) mediates 6-thioguanine genotoxicity by introducing single-strand breaks to signal a G2-M arrest in MMR-proficient RKO cells. Clin Cancer Res. 2003; 9:2327–34. [PubMed: 12796402]
27. Sengupta S, et al. Induced Telomere Damage to Treat Telomerase Expressing Therapy-Resistant Pediatric Brain Tumors. Mol Cancer Ther. 2018; 17:1504–1514. [PubMed: 29654065]

Europe PMC Funders Author Manuscripts

28. Mender I, Gryaznov S, Dikmen ZG, Wright WE, Shay JW. Induction of telomere dysfunction mediated by the telomerase substrate precursor 6-thio-2'-deoxyguanosine. Cancer discovery. 2015; 5:82–95. [PubMed: 25516420]
29. Valerie NC, et al. NUDT15 hydrolyzes 6-thio-deoxyGTP to mediate the anticancer efficacy of 6-thioguanine. Cancer Res. 2016
30. Nishii R, et al. Preclinical evaluation of NUDT15-guided thiopurine therapy and its effects on toxicity and antileukemic efficacy. Blood. 2018; 131:2466–2474. [PubMed: 29572377]
31. Almqvist H, et al. CETSA screening identifies known and novel thymidylate synthase inhibitors and slow intracellular activation of 5-fluorouracil. Nat Commun. 2016; 7:11040. [PubMed: 27010513]
32. Zhang JH, Chung TD, Oldenburg KR. A Simple Statistical Parameter for Use in Evaluation and Validation of High Throughput Screening Assays. J Biomol Screen. 1999; 4:67–73. [PubMed: 10838414]
33. Martinez Molina D, et al. Monitoring drug target engagement in cells and tissues using the cellular thermal shift assay. Science. 2013; 341:84–7. [PubMed: 23828940]
34. Pai MY, et al. Drug affinity responsive target stability (DARTS) for small-molecule target identification. Methods Mol Biol. 2015; 1263:287–98. [PubMed: 25618353]
35. Suiter CC, et al. Massively parallel variant characterization identifies NUDT15 alleles associated with thiopurine toxicity. Proc Natl Acad Sci U S A. 2020
36. Barretina J, et al. The Cancer Cell Line Encyclopedia enables predictive modelling of anticancer drug sensitivity. Nature. 2012; 483:603–607. [PubMed: 22460905]
37. Tzoneva G, et al. Activating mutations in the NT5C2 nucleotidase gene drive chemotherapy resistance in relapsed ALL. Nature Medicine. 2013; 19:368–371.
38. Hahn WC, et al. Creation of human tumour cells with defined genetic elements. Nature. 1999; 400:464–8. [PubMed: 10440377]
39. Page BDG, et al. Targeted NUDT5 inhibitors block hormone signaling in breast cancer cells. Nature Communications. 2018; 9:250.
40. Lee SHR, Yang JJ. Pharmacogenomics in acute lymphoblastic leukemia. Best Practice & Research Clinical Haematology. 2017; 30:229–236. [PubMed: 29050696]
41. Karran P, Attard N. Thiopurines in current medical practice: molecular mechanisms and contributions to therapy-related cancer. Nature Reviews Cancer. 2008; 8:24–36. [PubMed: 18097462]
42. Lim SZ, Chua EW. Revisiting the Role of Thiopurines in Inflammatory Bowel Disease Through Pharmacogenomics and Use of Novel Methods for Therapeutic Drug Monitoring. Frontiers in pharmacology. 2018; 9:1107–1107. [PubMed: 30349479]
43. Moriyama T, et al. Mechanisms of NT5C2-mediated thiopurine resistance in acute lymphoblastic leukemia. Molecular Cancer Therapeutics. 2019
44. Carter M, et al. Human NUDT22 Is a UDP-Glucose/Galactose Hydrolase Exhibiting a Unique Structural Fold. Structure. 2018; 26:295–303.e6 [PubMed: 29413322]
45. Gad H, et al. MTH1 inhibition eradicates cancer by preventing sanitation of the dNTP pool. Nature. 2014; 508:215–221. [PubMed: 24695224]
46. Jurrus E, et al. Improvements to the APBS biomolecular solvation software suite. Protein Sci. 2018; 27:112–128. [PubMed: 28836357]
47. Laskowski RA, Swindells MB. LigPlot+: multiple ligand-protein interaction diagrams for drug discovery. J Chem Inf Model. 2011; 51:2778–86. [PubMed: 21919503]
48. Winn MD, et al. Overview of the CCP4 suite and current developments. Acta Crystallogr D Biol Crystallogr. 2011; 67:235–42. [PubMed: 21460441]
49. Vagin A, Teplyakov A. Molecular replacement with MOLREP. Acta Crystallogr D Biol Crystallogr. 2010; 66:22–5. [PubMed: 20057045]
50. Adams PD, et al. PHENIX: a comprehensive Python-based system for macromolecular structure solution. Acta Crystallogr D Biol Crystallogr. 2010; 66:213–21. [PubMed: 20124702]
51. Painter J, Merritt EA. TLSMD web server for the generation of multi-group TLS models. Journal of Applied Crystallography. 2006; 39:109–111.

52. Jafari R, et al. The cellular thermal shift assay for evaluating drug target interactions in cells. Nat Protoc. 2014; 9:2100–22. [PubMed: 25101824]

53. O'Brien J, Wilson I, Orton T, Pognan F. Investigation of the Alamar Blue (resazurin) fluorescent dye for the assessment of mammalian cell cytotoxicity. Eur J Biochem. 2000; 267:5421–6. [PubMed: 10951200]

54. Yadav B, Wennerberg K, Aittokallio T, Tang J. Searching for Drug Synergy in Complex Dose-Response Landscapes Using an Interaction Potency Model. Comput Struct Biotechnol J. 2015; 13:504–13. [PubMed: 26949479]

55. Fedorov O, Niesen FH, Knapp S. Kinase inhibitor selectivity profiling using differential scanning fluorimetry. Methods Mol Biol. 2012; 795:109–18. [PubMed: 21960218]

Europe PMC Funders Author Manuscripts

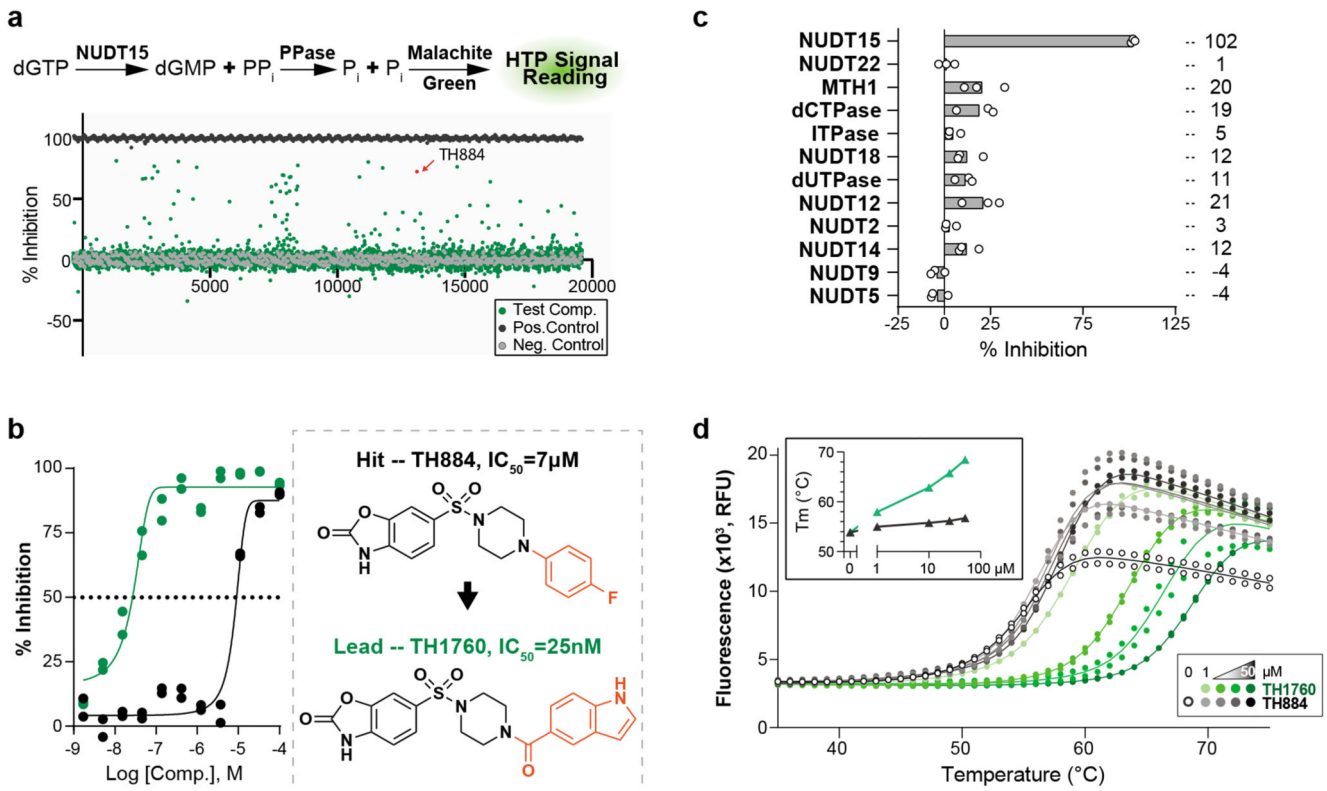

Fig. 1. Development of first-in-class NUDT15 inhibitor with nanomolar potency.

a. Screening campaign for putative NUDT15 inhibitor, utilizing an enzyme-coupled malachite green (MG) assay (upper panel), with the hit TH884 highlighted. **b**. Development from TH884 to the lead TH1760 with ~300-fold potency improvement, shown using MG assay. Inhibition% of n=2 experiments performed in duplicate shown. **c**. TH1760 was selective towards NUDT15, when assayed against other Nudix enzymes and/or pyrophosphatase at 100 μM. Mean inhibition of a representative experiment performed in triplicate shown, total of two experiments performed. **d**. TH1760 significantly stabilized NUDT15 from thermal denaturation in a dose-dependent manner, shown using DSF assay. Mean fluorescence signal (RFU) of a representative experiment performed in duplicates, with the melting temperatures in figure inset; total of two experiments performed.

Europe PMC Funders Author Manuscripts

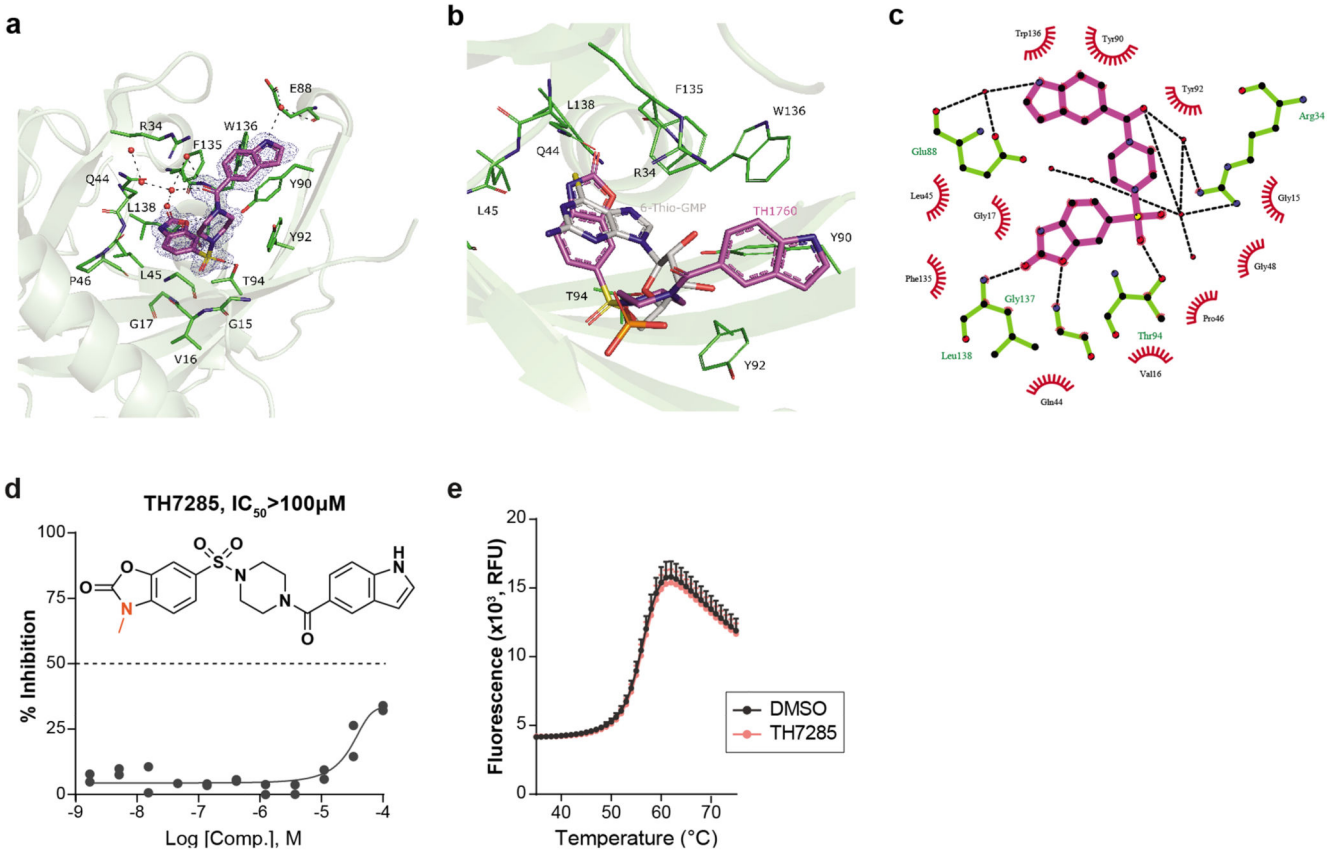

Fig. 2. Structural insight into NUDT15 inhibitor development

a. Close-up view of the binding interactions between TH1760 with NUDT15. Hydrogen bonds are shown in black and relevant residues are shown in stick representation. NUDT15 is shown in green, TH1760 in magenta and 2Fo-Fc electron density map around TH1760 in blue. **b**. Comparison of the binding positions of TH1760 and 6-Thio-GMP. Structurally aligned 6-Thio-GMP (PDB ID: 5LPG) is shown in grey. **c**. Ligplot+ representation of interactions between NUDT15 and TH1760, with hydrophobic interactions shown as an arc with spokes and hydrogen bonds shown as dashed lines. **d**. TH7285, a close analogue of TH1760, could not inhibit NUDT15, shown using MG assay. Inhibition % of n=2 experiments performed in duplicate shown. **e**. TH7285 minimally stabilized NUDT15 at 10 μM, shown using DSF assay. Mean RFU ± SEM of n = 3 experiments shown.

Europe PMC Funders Author Manuscripts

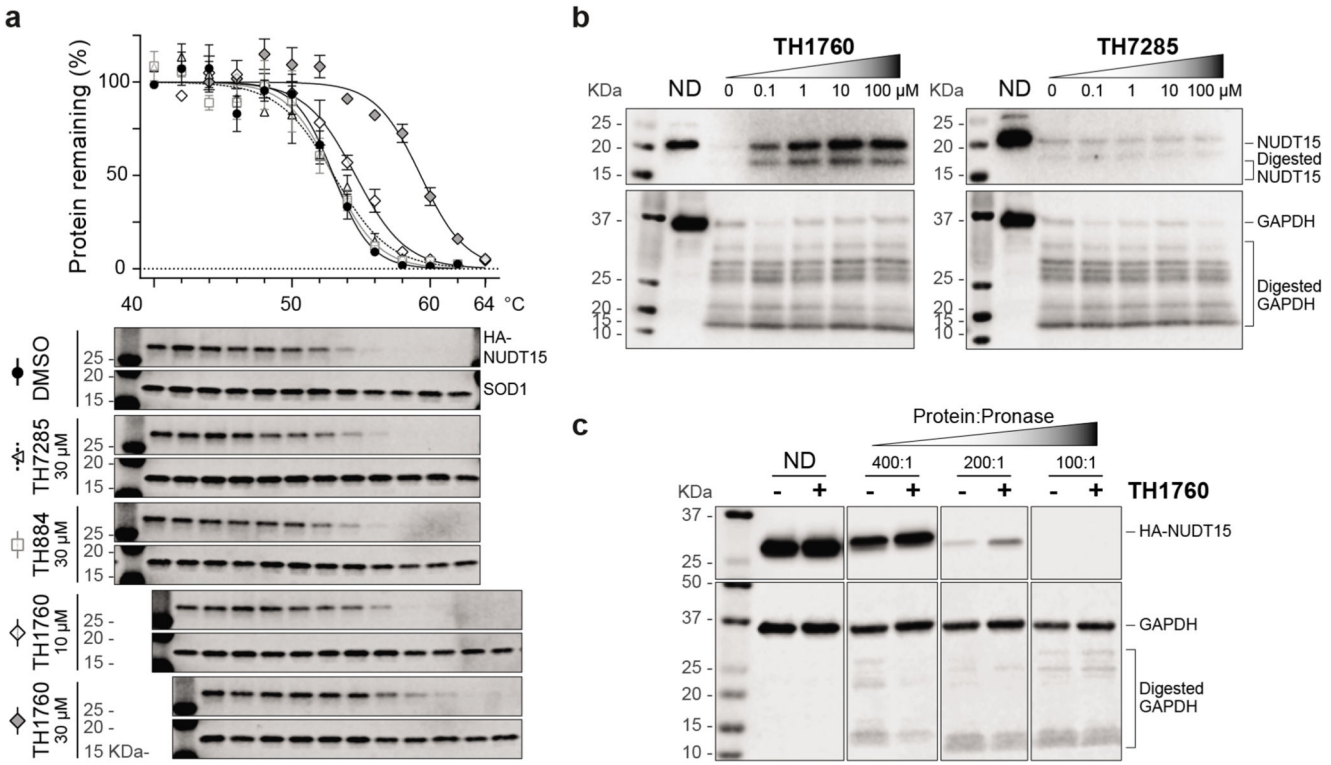

Fig. 3. TH1760, the lead NUDT15 inhibitor, displayed target engagement in cells.

a. TH1760, but not the hit TH884 or the inactive analogue TH7285, displayed target engagement in HL-60 overexpressing HA-tagged NUDT15. Compared to TH884 and TH7285, TH1760 substantially stabilized cellular NUDT15 from heat denaturation, demonstrated by CETSA. A representative Western blot shown in the bottom panel and mean band densities ± SEM of n = 3 experiments shown on top. Thermal stable protein SOD-1 served as the loading control. **b**. TH1760, but not TH7285, displayed target engagement using the orthogonal DARTS assay. Compound-treated lysates of U2OS cells were incubated with pronase solution or sample buffer (non-digestion, ND), followed by assaying for non-digested cellular NUDT15 *via* Western blot. GAPDH served as loading control. TH1760, but not TH7285, stabilized NUDT15 from pronase-guided digestion. **c**. TH1760 engaged and stabilized NUDT15 when applied to intact HCT116 cells. Intact HCT116 cells overexpressing HA-tagged NUDT15 were treated with 10 μM TH1760 for 4 h before been lysed and subject to DARTS assay. Protein lysate to pronase concentration ratios are indicated and GAPDH served as a loading control. Two experiments performed for b and c.

Europe PMC Funders Author Manuscripts

Europe PMC Funders Author Manuscripts

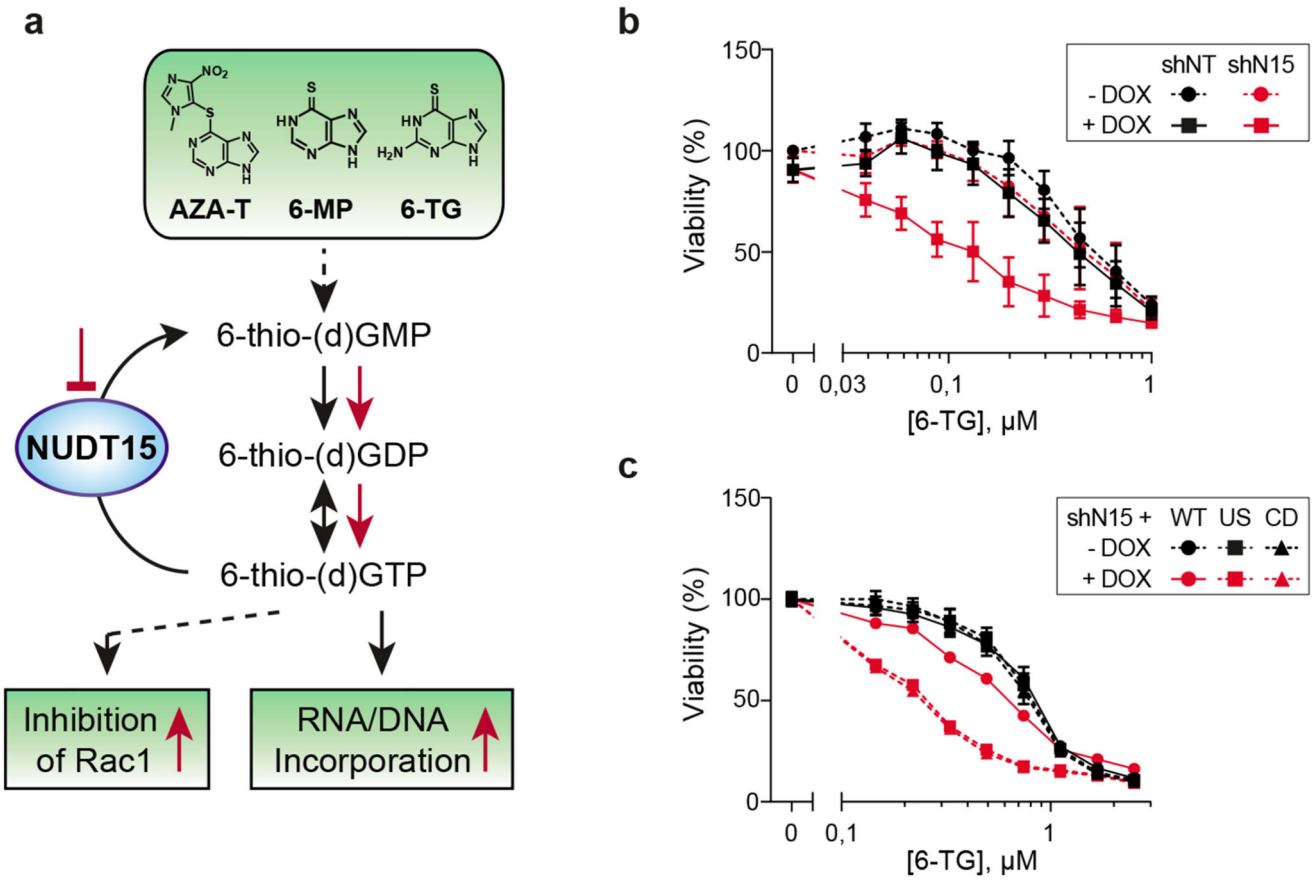

Fig. 4. NUDT15 inactivation potentiated thiopurine – a model for NUDT15 inhibitor evaluation.

a. Schematic drawing of thiopurine activation and metabolism. In cells, thiopurines (Azathioprine, AZA-T; 6-mercaptopurine, 6-MP; and 6-thioguanine, 6-TG) are converted into 6-thio-(d)GTP before being incorporated into the genomic material, and eventually cause cell death. NUDT15 limits thiopurine efficacy by converting 6-thio-(d)GTP into the non-toxic 6-thio-(d)GMP. **b**. Depletion of NUDT15 sensitized AML-derived NB4 cells to thiopurine treatment. Expression of NUDT15-specific shRNA (shN15), but not the non-targeting control shRNA (shNT), sensitized the cells to 6-TG treatment. Cell viabilities were determined using resazurin viability assay and calculated by normalizing to no doxycycline (DOX), DMSO-treated controls. Mean % ± SEM of n=3 experiments shown. **c**. NUDT15 enzymatic activity is the key in modulating thiopurine cytotoxicity in NB4 cells. NB4 cells co-expressing DOX-inducible shN15 and shN15-resistant, HA-tagged NUDT15 overexpression constructs (wildtype, WT; catalytically dead, CD; or unstable, US) were assayed for viability under 6-TG treatment. Only the expression of WT, but not CD or US NUDT15 protected cells from 6-TG. Cell viability % was assayed using resazurin viability assay and calculated by normalizing to DMSO-treated controls. Mean ± SEM of n=3 experiments shown.

Europe PMC Funders Author Manuscripts

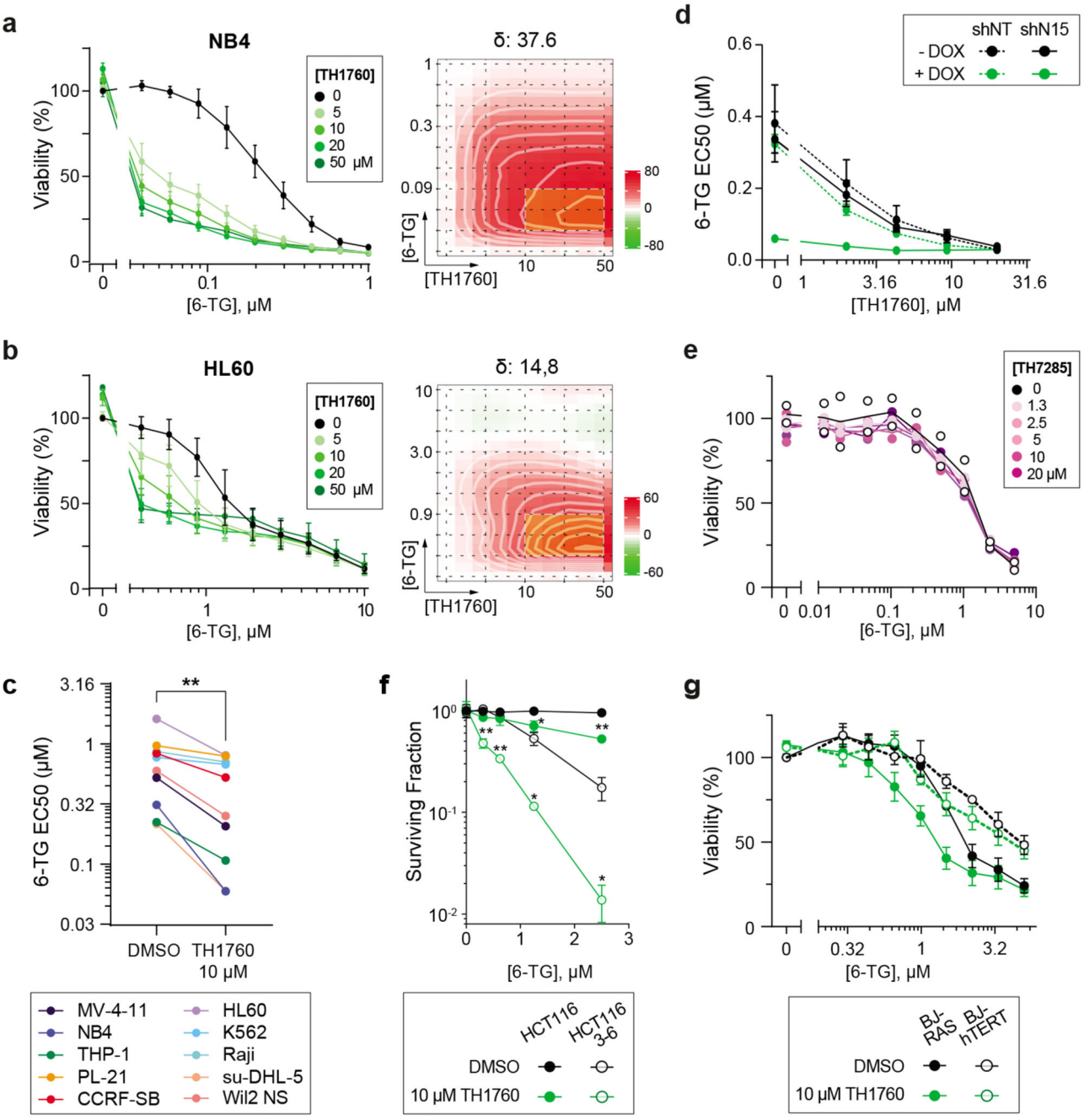

Fig. 5. TH1760 sensitized cells to thiopurine in a NUDT15-dependent manner.

a. **b**. TH1760 potentiated thiopurines in NB4 (a) and HL-60 (b)cells in a dose-dependent and synergistic manner. Mean viabilities ± SEM of n=3 experiments shown (left). Total synergy scores (δ) (right) of 6-TG/TH1760 co-treatment are shown with the dose-matrix in heat maps. **c**. TH1760 potentiated 6-TG in a panel of hematological cell lines. EC_{50} was determined by curve-fitting mean viabilities (n=3 experiments) using non-linear regression model; EC_{50}(6-TG only) Vs. EC_{50}(6-TG+TH1760), ** p=0.0013, t=4.582, df=9, 95% CI=0.3434~0.6961, r^2=0.6999, (two-tailed ratio paired t-test, Graphpad Prism). **d**. TH1760-

Europe PMC Funders Author Manuscripts

mediated 6-TG potentiation was abrogated upon NUDT15 knockdown *via* Dox-induced shRNA expression. EC_{50} shown with upper/lower limits were determined by curve-fitting mean viabilities (n=2 experiments) *via* non-linear regression model (Graphpad Prism). **e**. TH7285 did not potentiate 6-TG in HL-60 cells, upon co-treatment with 6-TG for 96h. Cell viabilities of n=2 experiments performed in duplicates shown, lines connecting means. **f**. TH1760 sensitized HCT116 and HCT116 3-6 cells to 6-TG, shown using clonogenic survival assay. Mean survival fraction ± SEM of n=3 experiments shown. Two-tailed t tests, DMSO Vs. TH1760 group: in HCT116, p=0.04 and 0.003 at 1.25 and 2.5 μM 6-TG; in HCT116 3-6, p=0.007, 0.001, 0.03, 0.02 at 0.3125, 0.625, 1.25 and 2.5 μM 6-TG. **g**. TH1760 preferentially sensitized tumorigenic BJ-RAS cells, versus the isogenic non-transformed BJ-hTERT cells. Mean ± SEM of n=3 experiments shown. Unless otherwise stated, cell viabilities were determined using resazurin viability assay and normalized to DMSO-treated control cells.

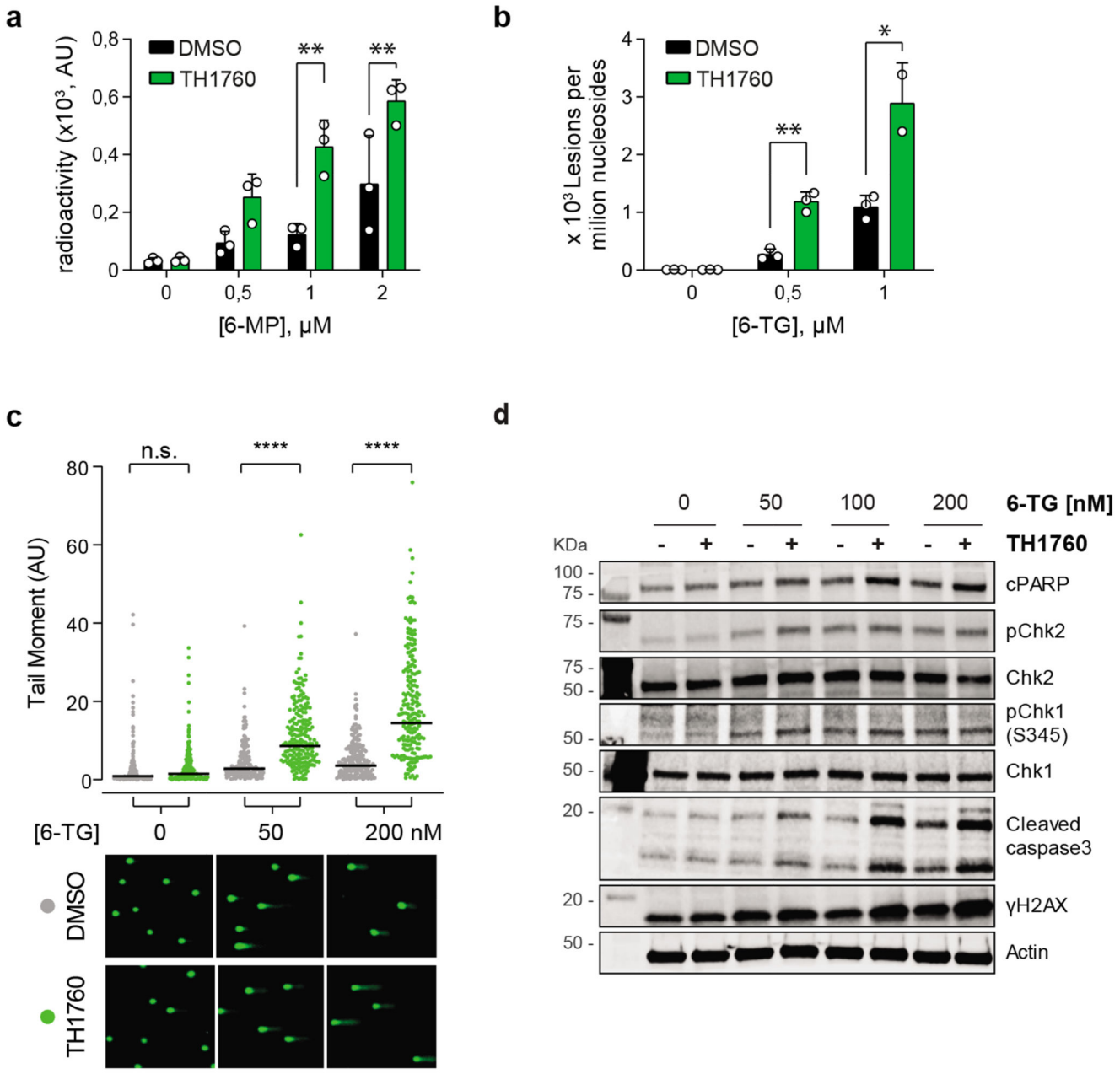

Fig. 6. TH1760 sensitized cells to thiopurines through promoting intracellular accumulation and incorporation of 6-thio-dGTP.

a. b. TH1760 significantly enhanced the intracellular accumulation and incorporation of thiopurines and their metabolites. HL-60 cells were treated with thiopurines alone or combined with 10 μM TH1760 for 16h, before levels of ^{14}C-labbeled 6-MP metabolite in DNA were determined *via* radioactive counts (a), or 6-thio-dGTP lesions in DNA were measured *via* mass spectrometry (b). Mean ± SEM of n=3 experiments shown. In a, DMSO Vs. TH1760 group: at 1 μM 6-MP, **p = 0.00027, t ratio=4.638, df=16; at 2μM 6-MP, **p = 0.00047, t ratio=4.381, df=16. In b, DMSO Vs. TH1760 group: at 0.5μM 6-TG, **p = 0.00117, t ratio=8.267, df=4; at 1μM 6-TG, *p = 0.02, t ratio=4.532, df=3. All performed

Europe PMC Funders Author Manuscripts

with multiple t-test (two-tailed, Holm-Sidak correction). **c**. TH1760 potentiated 6-TG-induced DNA damage in NB4 cells. NB4 cells treated with 6-TG alone or combined with 10 μM TH1760 for 48 h were assayed for DNA damage by alkaline comet assay. Top panel: Quantification of the tail moment of a representative experiment performed in duplicate (200 cells per condition). Lines represent geometric mean tail moments. DMSO Vs. TH1760 group: at 0 nM 6-TG, n.s., p=0.7054; 50 nM 6-TG, ****p < 0.0001, Z=9.652; 200 nM 6-TG, ****p < 0.0001, Z=11.78 (Kruskal–Wallis test, Dunn's correction, GraphPad Prism). Bottom panel: Representative, pseudo-colored images of treated NB4 cells following the alkaline comet assay. **d**. Western blot of DNA damage and apoptotic markers in HL-60 cells treated as described in c, confirming that TH1760 potentiated 6-TG-induced cellular responses. Two experiments performed.